FINITE ELEMENT ANALYSIS OF THE HUMAN FEMUR: A VALIDATION STUDY

PAUL M. SMITH

INFORMATION TO USERS

This manuscript has been reproduced from the microfilm master. UMI films the text directly from the original or copy submitted. Thus, some thesis and dissertation copies are in typewriter face, while others may be from any type of computer printer.

The quality of this reproduction is dependent upon the quality of the copy submitted. Broken or indistinct print, colored or poor quality illustrations and photographs, print bleedthrough, substandard margins, and improper alignment can adversely affect reproduction.

In the unlikely event that the author did not send UMI a complete manuscript and there are missing pages, these will be noted. Also, if unauthorized copyright material had to be removed, a note will indicate the deletion.

Oversize materials (e.g., maps, drawings, charts) are reproduced by sectioning the original, beginning at the upper left-hand corner and continuing from left to right in equal sections with small overlaps.

Photographs included in the original manuscript have been reproduced xerographically in this copy. Higher quality 6" x 9" black and white photographic prints are available for any photographs or illustrations appearing in this copy for an additional charge. Contact UMI directly to order.

Bell & Howell Information and Learning
300 North Zeeb Road, Ann Arbor, MI 48106-1346 USA

UMI®
800-521-0600

FINITE ELEMENT ANALYSIS OF THE HUMAN FEMUR: A VALIDATION STUDY

BY

©PAUL M. SMITH, B.SC, B.ED.

A THESIS SUBMITTED TO THE SCHOOL OF GRADUATE STUDIES IN PARTIAL FULFILMENT OF THE REQUIREMENTS FOR THE DEGREE OF MASTER OF ENGINEERING

FACULTY OF ENGINEERING AND APPLIED SCIENCE

MEMORIAL UNIVERSITY OF NEWFOUNDLAND

JANUARY 1999

ST. JOHN'S NEWFOUNDLAND CANADA

ABSTRACT

To facilitate improvement of hip replacement components and techniques, it is desirable to obtain calculated strains for typical loads that are accurate in an absolute sense. Finite element methods have traditionally been applied for this purpose, but in general results have proved useful only in a relative sense. This thesis outlines a semi automated finite element modelling method that accounts for both specific geometry and material properties of the femur under study and makes use of of computer tomography, and in-house designed modelling methods. In-house methods and software is used to convert raw computer tomography data into a finite element model with relatively little user intervention. To validate the modelling, calculated strains are compared to measured strains obtained from mechanical tests, which have also been carried out as part of this research. The mechanical testing is conducted under controlled environmental conditions which is a desirable feature. As well, material properties of the femur are experimentally investigated in a novel fashion that circumvents precision machining of the samples.

ACKNOWLEDGEMENTS

The author would like to thank Dr. J. Molgaard for acting as supervisor for the duration of this degree program. The guidance and support provided are greatly appreciated. Thanks are extended to the National Research Council of Canada, as well as the Faculty of Engineering and Applied Science at Memorial University of Newfoundland, through which funding was provided to carry out this research. Thanks to fellow graduate students, especially Ms. Dawna Greening, Mr. Chris Fowler, and Mr. Rodney Hale for helping to cope with the problems and frustrations encountered during this undertaking. In addition I would like to thank Memorial University, Biomedical Engineering Centre staff, John Tucker (project engineer) and Ron O'Driscoll (technical assistant). Without their help and expertise this project would not have been possible.

Contents

LIST OF FIGURES AND TABLES

Figures

Tables

NOMENCLATURE

Symbols

P	partial pressure of a gas
RH	relative humidity
P_o	partial pressure of pure water at temperature T
T	temperature
E	elastic modulus
E_c	elastic modulus of cortical bone
ϵ	strain
$d\epsilon/dt$	strain rate
ρ	density
ρ_c	density of cortical bone
θ_p	principle angle

Acronyms

FE	finite element
CT	computer tomography
PMMA	polymethlmethacrylate

CHAPTER 1

INTRODUCTION AND MOTIVATION

The Medical Engineering Group at Memorial University of Newfoundland has carried out preliminary work, to compare and contrast various designs of hip implants. Fibreglass femurs (Saw bones™ by Sawbones America Worldwide, ©1997) were sectioned, implanted, and mechanically tested, with strains measured at strategic locations. A human cadaver femur was also implanted and tested, again with strains measured. Phenomena such as stress shielding were verified and compared for various implants. Readers not familiar with the basic physiology of the human femur may consult Appendix D.

From this research the need was identified to develop a method of calculating strains in implanted human femurs, which takes into account differences in shape and mechanical

properties. This would facilitate comparing several different designs of implants. In addition, this method will make it possible to compare strains underneath the bone surface, and at interfaces; locations difficult or impossible to gather experimental data on. The problem is how to calculate these strains. Due to complexity in both geometry and material properties, analytic solutions are not feasible and numerical methods must be resorted to.

As is evident from the literature reviewed in Chapter 2, Finite Element Analysis (FEA) has become an accepted and widely used numerical tool in Biomechanics. However even after decades of use the method remains a challenge to apply. Due to the complex geometries involved, models are traditionally quite tedious and time consuming to construct. It is only in the past few years that automated methods have began to evolve. This is of course linked to order of magnitude increases in computer processing power and advances in medical imaging and image processing.

The common practice in Biomechanics laboratories is to develop in-house software that links together various commercial software packages (ie. image processing, solid modelling, and Finite Element). The in-house software, being dependent on the commercial software, computer hardware, and medical imaging facilities available to a particular laboratory, renders the software difficult to transfer unless another laboratory possesses identical resources. The field is not sufficiently mature that off the shelf technology is available.

The specific purpose of this project was to develop technology, utilizing the available commercial software, computer hardware, and medical imaging resources available to Memorial University of Newfoundland to build FE models of human femurs. An emphasis was placed on two essential areas. First, an effort was made to both model and mechanically test the femur in a configuration that is physiologically realistic. The challenge was to achieve this while not sacrificing reproducibility and consistency of results. Secondly, the intention was to base material property assignment on Computer Tomography (CT) data and not on literature values or other laboratories' data sets. CT allows the analyst to account for the nonhomogenious nature of bone at least down to the resolution of the particular scanner being used. Most importantly, the criteria that relate material properties to CT numbers was to be calibrated and validated in this laboratory.

The purpose is to provide Memorial's Medical Engineering with a numerical tool to explore the hip replacement question even further. As well contributions will be made to the Biomechanics field in general. Individual specimens will be modelled closer to physiological conditions and with material properties more accurately represented.

CHAPTER 2

FINITE ELEMENT ANALYSIS OF THE HUMAN FEMUR: A LITERATURE REVIEW

2.1 Introduction:

For the past two decades, the finite element method (FEM) has been utilized extensively in biomechanical studies, with the human femur receiving the most attention. One might think that because of the femur's prominent position among FE studies, little room would remain for further research. While there has been progress and much has been learned, the field is still rather immature when compared to other areas of FE analysis. This immaturity is essentially due to bone complexity, both in terms of geometry, and material

properties.

To have any quantitative confidence in the FE method applied to a complex material such as bone, results must be validated experimentally (ie. mechanical testing must be used to verify the FE model). There have been hundreds of papers published concerning use of the FE method to calculate stresses in the human femur, as well as human femurs with prosthetic implants, and model femurs (made from epoxy or fibreglass). As far as the author is aware only Valliappan et al., (1977); Svesnsson et al., (1977); Tar et al., (1980); Hampton et al., (1980); Rohlman et al., (1982); Lewis et al., (1991); Harrigan et al., (1992); Verdonschot et al., (1993); Tanner et al., (1995); Leone et al.,(1990); Lewis et al., (1981); Lotz et al., (1991); and Keyak et al., (1993) validate their results through mechanical testing. These papers are reviewed here in detail but first the field is reviewed in more general terms.

2.2 Field in General:

Starting in the late 1970's several papers were written that put FE studies of the human femur and human bones in general on a somewhat secure foundation (Svesnsson et-al., 1977; Valliappan et al., 1972; Tarr et al., 1980 and Rohlmann et al., 1983). Generally these investigations found good correlations between mechanical testing results and FE results, at least in a relative sense. Relative sense means that trends in the stress patterns

were similar in the FE and mechanical results. In an absolute sense the results were generally poor. To investigators and designers working with hip prosthesis an analytic method that promised good results, even in a relative sense, was a huge step forward. Other numerical and analytic methods had proved totally inadequate while mechanical testing was expensive, time consuming and for some types of problems impossible.

Early prosthetic hip implants were for the most part cemented. The most critical problem for this type of implant involved failure of the cement layer itself. For this reason early optimization attempts involved reducing stress in the cement layer. This problem was ideally suited to FE analysis (in its state of development at that time) because when the goal is to achieve the lowest stress possible, relative stress fields are sufficient. In addition, actual mechanical measurement of stress in the cement layer is technically difficult even in today's context. O'Connor et al., (1996) and Burke et al., (1984) have claimed some success in this regard.

The medical and engineering communities soon learned that minimization of cement stresses would come at a cost. Reducing stresses in the cement layer enhances a phenomena called stress shielding. Since the prosthetic stem is stiffer than the surrounding bone it tends to shield the surrounding bone from loading at the hip joint. Shear stresses in the cement layer would transfer some of this load to the surrounding bone and keep stresses in the bone at least near the physiological level. The risk is, that the cement will fail in shear stress and result in all the load being carried by bone near the

tip of the implant with very little load transferred to surrounding bone. Bone shielded from stress resorbs from disuse (atrophy) while the bone at the tip of the femur would become more dense from overuse (hypertrophy). As with most engineering problems optimization of design parameters is a delicate balance. The cement layer must be stressed to a level that maximizes load transfer to the surrounding bone (ie. reduce stress shielding) while reducing risk of failure in the cement layer itself. Early studies such as Kwak et al., (1979); Hampton et al., (1979); and more recently Yoon et al., (1989); Janson et al., (1993); Harrigan et al., (1991) have focussed their efforts primarily on optimization of the cement layer.

The overall process of cement failure, stem loosening and bone resorption manifests itself clinically as either a painful or totally failed implant. The operative procedure may have to be repeated and with the head of the femur in a much worsened condition then it would have been for the original procedure. A high percentage of hip replacements fail completely or become unbearably painful within ten years. The clinical goal of applying FE analysis to hip prosthesis is to increase the life expectancy of the implant and therefore reduce the number of repeat operations. This is quickly becoming a very important issue as the hip replacement procedure is applied to younger and more active people.

The FE method of analysis is quite useful in finding a balance between cement layer stress and stress shielding of the surrounding bone. Relative stress fields may suffice in

this regard. Also there is no experimental method for measuring stresses underneath the surface of the bone where the most significant stress shielding occurs. It is also worth noting that up to the present no calculated FE stresses have been verified anywhere except on the surface of the femur (as far as the author is aware). Researchers have assumed that verification of stresses in a relative sense on the surface of bone is enough to warrant the use of FE to calculate stresses at all locations in the femur within the context of parametric studies.

In more recent years press-fitted implants have been used. Press-fitted implants are designed to produce hoop stresses in the surrounding bone and therefore reduce stress shielding. The idea is to transfer load to the surrounding bone. Porous coatings have also been used in an attempt to transfer load (via shear stresses) along the implant surface. The role of the porous coating is to stimulate bone ingrowth so that subsequently the interface may transfer shear stresses. FE methods have been extensively applied to this form of implant (Skinner et al., 1994; Keaveny et al., 1993; Kang et al., 1993; Huiskes 1990 and Harrigan et al., 1991), but little experimental verification has been carried out. Most of the comparison studies have been on either intact femurs or femurs with cemented implants.

FE has also been used in attempts to simulate bone remodelling (absorption due to disuse or hypertrophy due to overuse). Essentially these are time step algorithms that utilize FE to calculate the stress field in each time step. Material properties are changed as a

function of the stress field and then of course the stress field must be recalculated because of the change in material properties. Each cycle in this process corresponds to a specified period of real time that depends on the bone remodelling theory being used. Years of bone loading can be simulated in minutes on a computer. Beaupre et al., (1990); Skinner et al., (1994); Rietbergen et al., (1993); Weinans et al., (1994); Carter et al., (1989); Huiskes et al., (1992); Sumner et al., (1992) and Fyhrie et al., (1995) have explored this area. It is obvious that these sort of calculations are extremely difficult to verify. One study (Skinner et al., 1994) compared x-rays of patients taken shortly after surgery with x-rays taken at later times. This is the only verification of which the author is aware. Schmalzried et al., (1992) studied implanted femurs retrieved at autopsy and observed evidence of bone remodelling. No comparison with remodelling equations was attempted. Alberts et al., (1993); Bobyn et al., (1992) and Goldstein et al., (1987) performed animal studies where bone remodelling was observed. In all, there is not much to support remodelling algorithms in a quantitative sense. Considering, that the FE part of the algorithm gives only relative stress fields, it is difficult to imagine the overall process being accurate in any absolute sense. To pursue these sort of simulations, an absolutely accurate method of calculating stress fields is needed. Of course FE holds the most promise as long as techniques can be improved to get experimentally verifiable stress fields. More work is needed in this regard.

If stresses could be calculated accurately in an absolute sense it would make FE a much more powerful tool for the testing and design of prosthetic implants. Cement stresses

could be calculated for various loadings and compared with strength data for cement. Stress fields in surrounding bone could be used (in tandem with reliable remodelling equations) to accurately predict the degree to which bone remodelling would occur. These factors directly influence the life span of the implant and are therefore extremely useful to know. In addition CT scans can be taken in vitro (providing data for FE analysis) allowing FE calculations to be used in such areas as fracture risk assessment . Lotz et al., (1991a) pursued a FE study of the human femur with the long term goal of fracture risk assessment, and to learn more about the consequences of bone pathologies such as osteoporosis and metastatic lesions. This study was followed up by an attempt to take into account the non-linear material properties of bone (Lotz et al., 1991b). In general FE techniques accurate in an absolute sense will be very useful in ways we can imagine and even in ways we might not imagine at this time.

It would also be very useful if the FE model construction process for bones could be improved. Presently we have available to us imaging technology such as CT scans that provide automatically all the raw data needed to build extremely precise FE models at least from a geometric perspective with the probability that material properties can also be modelled. CT "density" numbers, based on extent of X-ray photon absorption, can be determined accurately at each pixel location within a CT scan image with the distance between pixels being less than a millimetre. The hope is that material properties can then be assigned to FE models based on bone density which can be predicted from CT numbers. Rho et al., (1995); Keyak et al., (1990) and Keaveny (1993) describe how bone

density may be computed from CT numbers. Essentially, all claim a linear relationship between bone density and CT number. Rho et al. verified this experimentally but found a better correlation for trabecular bone then for cortical bone. A linear calibration is then derived from two reference points in one of the CT scan slices. Keyak et al. uses water and cortical bone itself which has a relatively consistant density of 1.8 g/cm^3. The relationship between bone density and CT numbers as well as published relationships between bone density and material properties will be discussed under a separate heading later in this chapter.

A major difficulty is that CT scan output files are simple lists of numbers that must be processed to facilitate transfer of the data to commercially available FE software. To fully utilize the degree of resolution contained in the CT scan output, an FE model would have at least thousands and maybe tens of thousands of nodes. Inputting coordinates manually is at best extremely tedious and time consuming. Software needs to be developed that bridges the gap between CT scan output and FE input. Keyak et al., (1990); Bartel et al., (1990); Edidin et al., (1991) and Lengsfeld et al., (1994) have made progress in this direction but not much technical detail is given in their publications. Reseachers tend to use their own in-house software in conjunction with commercially available software. Having said this, informal correspondence with various researchers confirm the author's suspicions that building these models remains to date a time consuming and tedious procedure.

2.3 Experimental vs Finite Element Results:

It is clear from looking at the field in general that there is a need to verify the results of FE studies quantitatively. New initiatives such as fracture risk assessment and bone modelling studies have increased the importance of this. In this section, the author will review in some detail studies in which FE results have been verified via mechanical testing. Experimental procedures as well as FE techniques are discussed. The author has determined informally (via email correspondences, and monitoring of Biomechanics list server) that the most prominent sources of error in FE simulations of biomechanical experiments are: (1) Matching of boundary conditions (loads and restraints) between the FE model and the experimental configuration, and (2) Assignment of material properties in the FE model. Bone is anisotropic and non-homogenous, making it extremely difficult to model. There is also a significant variation between specimens. This means there is no one modulus describing the elastic properties of bone. These issues are given special attention below.

Valliappan et al. first compared FE results to mechanical testing (Valliappan et al., 1977). The specimen was a cadaver femur, modelled from midshaft upwards. The FE model consisted of eight noded linear isoparametric elements. These elements have eight arbitrarily located corner nodes with eight warped faces. The software was in-house, designed by the authors and run on a 360/50 computer. Four models with varying

degrees of mesh refinement were used. Mesh density ranged from (92 elements-152 nodes) to (196 elements-323nodes). This mesh would be considered extremely coarse by todays standards but probably utilized the authors' full computer capability in 1977. There is no explanation of how the femur geometry was determined and digitized for FE input. All materials were considered to be homogeneous, linear and isotropic and elastic moduli for both cortical and trabecular bone were taken from previously published literature. This introduces substantial error since there is significant variation in material properties from one femur to another. In addition bone is neither homogeneous, linear or isotropic.

Experiments were carried out on a single cadaver femur. The load was applied to the head of the femur, directed toward the intercondylar notch. No muscle forces were applied. Strains were measured with an extensometer and loads with a force gage. The extensometer was used at various angles so that principle strains could be calculated. The author claims good comparison of experimental and FE results on the lateral boundary of the shaft with some discrepancy in tensile strains. Judging from the graphs provided with the paper, the only reasonable results obtained were on the lateral side of the shaft. It is difficult to determine percentage differences from the information provided.

The authors proceed to investigate walking cycle and static posture with the same FE model. The results of this further investigation are no longer of much value, considering the previous results and the complex loading conditions now being considered. Not-

withstanding, this paper is pioneering work on FE analysis of the human femur.

In the same year the same authors Svesnsson, Valliappan and Wood published a second paper entitled "Stress analysis of human femur with implanted Charnley Prosthesis" (Svesnsson et al., 1977). As is obvious from the title this time the analysis involved an implanted femur. The authors state that although a 3-D FE analysis would be desirable, the number of elements would exceed their computer resources. For this reason the authors proceeded with a 2-D analysis. From the onset it was made clear that they only intended to calculate stresses in a relative sense. To compensate for the 2-D model side plates were used to factor in the contribution from the portion of the cortical shell outside the 2-D slice being modelled. This technique was common in early FE studies. In this study the FE model geometry was obtained by physically slicing the femur and taking measurements manually. Again published literature was used to set material properties in the FE model. No attempt was made to measure the actual material properties of the specific bone being analysed. The objective of this study was to calculate the stresses at the interfaces of different materials within the structure (ie. bone-cement and cement-metal). These stresses impact on the problem of stem loosening. Convergence of the model was established via a finer mesh and validation was attempted by comparing results with mechanical testing previously carried out by Brochurst (1975). Brochurst had mechanically tested a similar bone with a similar prosthesis and a similar load (single joint load). He measured surface strains and calculated principal strains. Svesnsson et al. compared their calculated strains with Brochurst's measured values and found in their

own words "qualitative similarity in the distribution". This is the best that could be expected considering both the crudeness of the FE model and the follow up comparison. However this is a pioneering study and did serve to identify regions of maximum and minimum stress in the bone-cement-prosthesis structure. It was concluded that a heavier prosthesis would reduce maximum stresses in the cement layer. What was not realized at the time was that reduction of stress in the cement layer would contribute to stress shielding.

In 1980 Tar et al. performed a 3-D FE analysis of a natural femur and also a femur with several different prosthetic designs implanted (Tar et al., 1980). The FE model consisted of 8-noded isoparametric hexahedral elements. Geometry and material boundaries were determined by physical sectioning of the femur. Internal and external boundaries as well as spatial variations in both cortical and trabecular bone were taken into account. The mesh was generated on an interactive computer graphics finite element preprocessor. All materials were assumed linear elastic and isotropic and material constants were taken from the literature. Interfaces were assumed to be perfectly bonded (ie. no slipping or coulomb friction at boundaries). In total four meshes were generated, one for the natural femur, and one for each of the implanted femurs. Mesh density ranged from 891 elements to 1032 elements. There was no insurance of a converging solution since only a single mesh density was used per structure.

Mechanical testing was carried out on an implanted femur instrumented with 13 strain

gages. The distal third of the femur was sectioned and the remaining proximal portion potted vertically in a cylindrical steel base support. Only a single joint reaction force was simulated by the loading jig.

Tar et al. claims satisfactory correlation of strain data with the FE results. He claims only 10% discrepancy along bone surfaces if one of the gages is neglected. Strains in the stem of the prosthesis were off by 60%. Over all only general trends in stresses were satisfactorily modelled.

In 1980 Hampton et al. carried out a 3-D FE analysis of a human femur implanted with a Charnley prosthesis (Hampton et al., 1980). Again three dimensional isoparametric hexahedral elements were used and all materials were assumed to be linear, isotropic and homogeneous. Loads were applied at the ball of the stem with no attempt made to model muscle forces. Material constants were obtained from the literature. The FE mesh was very coarse with only 31 elements comprising the entire structure. There is no mention of how geometry or material properties were obtained.

Results from the FE calculations were compared with experimental work done by Andriacchi et al., (1976). Only agreement in terms of general trends was claimed. There was close agreement on the location of maximum stress. This model with its extremely coarse mesh would be considered quite crude by today's standards.

Rohlman et al. did an in-depth analysis of the femur, with and without endoprosthesis (Rohlman et al.,1982) . The FE model consisted of 1950 isoparametric 8-noded brick elements. Only one model was constructed, therefore no proof of convergence was possible. Geometry was obtained by embedding the femur completely in epoxy resin and sectioning it into 38 slabs. Each slab was x-rayed and areas of equal density were identified. Elastic modulus was assigned based on material density within a specific region. It is not clear from the paper what the spatial resolution was in density measurements. This is a significant refinement over previous studies in which material moduli were taken from published literature. As previously stated, no two femurs have the same geometry or the same spatial distribution of material properties. This was the first attempt to take into account the inhomogeneous nature of the bone. All materials were however, considered to be linear elastic and isotropic. The model was loaded with both a joint reaction force and an abductor muscle force.

Physical testing was carried out on a cadaver femur. Loading, with both a joint reaction force and an abductor muscle force, was made possible by an in-house designed jig. While the load was applied strains were measured via 34 rosette strain gages attached to the femur surface. The lower end of the femur was embedded in a block of aluminum.

The authors do not quote any percentage differences between their experimental and FE results. They state that good results were obtained in a relative sense. This can be seen from the bar charts of measured and calculated strains, included in the published paper.

In an absolute sense the results are considerably different. The authors conclude that FE is useful only in parametric studies, and not very useful if absolute stresses are required. These are reasonable conclusions for a study that was "state of the art" at the time.

Lewis et al. did a FE analysis of an epoxy composite, full scale model of the human femur. The model was CT scanned and the data used to build a 3-D FE mesh (Lewis et al., 1991). The load in both the physical test and the FE model simulated the single leg stance (338 N joint reaction force on the femoral head and 111 N abductor muscle force on the greater trochanter). A torsion load of 156 N was also applied which represents the hip being flexed 90°. Data was collected via four rosette strain gages located medially and laterally on the femur surface.

The authors claim good correlation between FE and experimental results. Unfortunately, very little detail is provided on the FE analysis (mesh density, element type, etc). There are however, three very important points that emerge from this relatively simple study. Firstly, the authors state that the measured strains are extremely sensitive to the degree of abduction. This emphasizes the need to include abductor muscle forces in testing. FE models must be able to model and account for abductor muscle forces. Modelling and testing with joint reaction forces only is obviously a simplification of the physiological reality. Secondly, the geometric accuracy and the mesh design has substantial impact on results. This emphasizes the importance of developing an accurate method of reproducing the geometry (for FE mesh) of the specific human femurs being tested.

Finally, the authors suggest using 2-D plate elements to simulate strain gages on bone surfaces. I am not aware of this ever being done and it might be very useful in accounting for the strain gage material backing. Strain gages are designed primarily for testing on surfaces which are much stiffer that the backing material on the gage itself. This is not necessarily the case with bone.

Harrigan et al. did an analysis that focused primarily on stresses in the cement layer of a cemented prosthesis (Harrigan et al., 1992). During the implantation strain gages were embedded in the cement matrix at six different locations. No detail is provided on this process other than a reference to Burke et al., (1984). In addition rosettes were mounted at three locations on the medial and lateral aspects of the femoral shaft: just below the prosthesis collar, halfway down the prosthesis, and at the level of the prosthesis tip. The femur was loaded in a configuration, simulating a one legged stance, including both joint reaction and abductor muscle forces. The tests were performed using a Materials Testing System servo hydraulic test machine. Loads simulating stair climbing were also investigated.

After testing, the femur was embedded in a rectangular block of resin and sectioned at 5-mm intervals in the transverse plane. The edges of the block were used as a coordinate system for FE mesh generation. Calibrated photographic enlargements were used to guide tracing of the geometry so that the anatomy of the femur could be carefully and accurately reproduced. Tracings made from the enlargements were digitized and used in

tandem with in-house software to generate the 3-D FE mesh.

Two FE meshes were generated. The first consisted of 345 elements modelling the prosthesis, 1142 elements modelling the bone cement, 344 modelling the trabecular bone and 1114 modelling the cortical shell. This is a total of 3800 nodes. The second model has a proportionally increased number of elements in all components for a total of 10000 nodes. The use of two meshes, one finer than the other allows the researcher to determine if the FE solution is converging. The FE elements used were 3-D linearly interpolated solid elements. Materials were assumed to be both linear and isotropic. The published paper includes several figures that illustrate the meshing pattern at several cross sections.

Harrigan et al. give relatively detailed comparisons between their experimental and FE results. Discrepancies between FE and experimental values at gage locations within the cement mantle range from 10 to 40 percent. With regard to the other gages, results are relatively similar (both show stress shielding etc). The results with the finer mesh were not significantly better than those with the courser model. This means that the coarser mesh was adequate and the finer mesh was a waste of generation time and computer time. The authors suggest that results might be improved by the use of non-linear contact elements at material interfaces and suggest they may attempt this in future work.

To summarize, this study is more narrowly focused than most but reveals some promising techniques for determining geometry and FE mesh generation. On the negative side there

was no mention of material properties being measured for the particular femur under study. Typical values taken from the literature were used. If x-rays instead of photographs were used, femur geometry and bone densities may have been determined without much additional effort.

Verdonschot et al., (1993) did an FE analysis and compared it with experiments done previously by Carlsson et al., (1988); and Tanner et al., (1988). Carlsson et al. conducted a load transfer experiment with loads simulating the one legged stance (abductor muscle and joint reaction forces included). Stress data was gathered by placing a pressure sensitive film between the medial edge of the prosthesis and the inner aspect of the femoral neck. Tanner et al. did a rotational stability experiment in which the rotational relative motion between the prosthesis and bone was measured. The loading involved cyclic anterior/posterior directed forces of 400 and 800 Newtons on the femoral head.

The FE model consisted of 1052 eight noded brick elements with 1600 nodes. Four different materials (linear and isotropic) were used with values for moduli taken from previous studies. No attempt was made to determine the material moduli of the specific femurs being studied. This paper does not explain how the geometry of the femurs was determined or how the FE mesh was generated.

The results of FE calculations and experiments are compared by ranking the stresses (ie. % of nodes with a stress value within a specified range). In this fashion the results

compared rather well. Of course, this shows that the stresses are similar only in a relative sense. The authors state that "Differences in an absolute sense are obvious and unavoidable". They claim idealized interface conditions are the major culprit in this regard. As an example, perfect prosthetic fit was assumed in the FE model. This is probably never realized either experimentally or clinically. This source of error may indeed prove very difficult to overcome, but might be insignificant when compared to error generated by inaccuracies in material properties and boundary conditions.

A quote from Verdonschot et al. may serve to highlight the importance of FE studies and the need to improve FE techniques:

> "FE simulations as a pre-clinical test procedure have the capacity to perform several tests with the same model (as shown here) and produce any relevant stress, strain or relative motion variable desired. In most cases it is practically impossible to assess these variables experimentally. The present study indicates that computer simulation studies with FE models can produce results that are similar to those of laboratory tests. Even more importantly, the conclusions drawn from the experiments are the same as those drawn from the FE analysis, meaning that this information could have been available even before prototypes of the designs were made."

Tanner et al. specifically investigated the effect of stem length in an uncemented

endoprosthesis (Tanner et al., 1995). The FE model was 2-D and consisted of quadratic isoparametric elements, both eight noded quadrilaterals and six noded triangles. Three models were created, each with different stem lengths, and numbers of elements ranging from 1095 to 1206. Materials were assumed to be linear elastic and isotropic, however non-linear gap elements were used to model the bone prosthesis interface. The authors give no indication of how material properties or geometry were determined.

Two prosthesis were mechanically tested, one with a full length stem and one with a shortened stem. Applied loads simulated a one legged stance, including abductor muscle forces. Stresses were measured at the bone prosthesis interface using a composite wafer of pressure sensitive medium grade Fuji pre scale film. Stresses were determined from colour changes in the film.

Quantitative comparisons of FE and mechanical testing results were poor. The authors claim that they were only interested in relative effects and absolute results were not important. No details regarding the magnitudes of results are given. This was essentially a parametric study with no attempt to quantify a comparison of FE and experimental results.

Keyak et al. attempted to validate their newly developed automated FE technique (Keyak et al., 1993). The technique involves utilization of a CT scanner, in-house software, and ABAQUS (a commercially available FE program). The in-house software is used to

convert raw CT data to a form that is readable by ABAQUS. The automatically generated mesh consists of cubes which as close as is possible approximates the geometry of the bone. In this validation study the automatically generated mesh contained 17244 nodes and 13778 elements. The linear isoparametric cube elements were 3-mm on a side. The in-house software also uses the CT data to assign an elastic modulus to each element that composes the model. In this way the inhomogeneity of the material can be modelled with greater resolution than it as been in any other study to date. However there are disadvantages to the technique. Using all cubes means that a very fine mesh must be used to closely approximate the bone geometry. Because of this, huge chunks of computer time and memory are needed for analysis. In addition the surface of the model is irregular. Inside and outside corners are unavoidable when modelling with cubes. These corners will result in stress concentrations that do not exist in the real femur. Keyak et al. counter this argument by stating that the stresses of primary interest are actually located underneath the surface. They claim that the stress concentration problem is a non-issue.

The experimental portion of this study is described in detail in the paper. Eleven strain gage rosettes were attached at various locations along the shaft and neck of the femur. The process of attaching the gages is described in detail. The base of the femur was embedded in polymethlmethacrylate (PMMA). The femur was loaded in compression (no abductor muscle force) in an electro hydraulic materials test system. The load was applied by two parallel plattens, one supporting the PMMA base and the other pressing

on the cartilage of the femoral head. This load was modelled as a point load on the ball of the femur and full restraint where the shaft enters the PMMA base. This is not entirely accurate since the bone may deform where it enters the base. In addition a platten does not apply a point load. A displacement boundary condition might have been more appropriate. A system of grids marked on the femur were used to locate gages and correlate the experimental data with points in the FE model. The grid was also used to accurately determine the loading direction.

To compare experimental results with FE results, a regression analysis was carried out. It was shown that the FE results were a valid predictor of the measured strains ($p<0.001$) This says nothing about the magnitude of the results, but rather it shows that they are the same in a relative sense. The standard error was between 254 and 311 micro strain depending on how the regression is carried out (experimental predicting FE or FE predicting experimental). This is a significant error in an absolute sense. The authors include a table showing the measured and FE strains at all eleven gage locations.

It is important to note that the FE mesh generated and used in this study is very different than that utilized in any other study reviewed. The mesh was generated automatically from raw CT data with little human intervention. While the mesh is extremely fine (ie. very large number of elements), in another way it is quite crude. FE models that simulate complex geometries are generally not composed of perfect cubes. Engineers use judgement, experience, and intuition when designing meshes of complex structures such

as femurs. Element shapes that relate in some meaningful way to the overall structure are used. It is very challenging to program computers to carry out this task appropriately. It is certainly desirable to generate FE meshes automatically and Keyak et al. have made a significant contribution. However much more work needs to be done towards developing software that mimics the skill and judgement of the experienced engineer.

In 1981 Huiskes et al. performed an extremely detailed experimental analysis of the human femur (Huiskes et al., 1981). Although the experimental results are not compared to FE results, their work will be reviewed because it highlights important experimental techniques and is one of the most detailed experimental studies ever carried out. In addition it emphasizes the importance of treating bone as an anisotropic material.

Both femurs of a 52 year old male were used. One was used for testing and the other was used to determine geometry. One hundred strain gage rosettes were attached to the test femur, 3 elements each in a rectangular configuration. The distal end of the bone was fixed in a steel box (no detail on how this was done) and the femur head was fitted with a brass cap to facilitate the application of load. Twelve different loads were applied to the femoral head, positive and negative forces in three directions as well as positive and negative couples in three planes. Strain measurements began three minutes after the application of each load to allow viscous effects to subside. The data acquisition rate was 2Hz (a detail not typically reported by other investigators), and a low excitation voltage (1.25-V) was used to avoid local heating of bone from the strain gage. After

experimental testing of the intact femur, the same femur was tested in the same fashion with three different types of prosthesis implanted.

Measured strains were compared with values calculated by 3-D beam theory. The results were particularly good in the shaft area when the anisotropic nature of the bone was taken into account.

The other femur (not tested) was embedded in Araldite (an epoxy cement) and sliced into thirty sections. The bone contours in the sections were digitized and the resulting data was used to determine the geometry of the femur. The right femur was assumed to be a mirror image of the left.

Leone et al. point out that it is difficult to validate FE models of press fitted implants because the bone ingrowth, necessary for proper function of the implant is impossible in cadaver specimens (Leone et al., 1990). An epoxy composite femur, which supposedly simulates bone ingrowth was mechanically tested and modelled. The epoxy femur was scanned and the CT data was used to construct a FE mesh. The scan slices were hand traced and digitized. This is obviously not making the best use of CT data which is already digital and contains all geometric information necessary to construct the mesh. In-house software was then used to convert the digital data to a form compatible with PATRAN which is a commercially available FE package. Material properties were assumed to be isotropic and linear. Boundary conditions were in the form of point loads

on the ball and greater trochanter with magnitudes of 75 and 25 lbs. respectively. This simulates the basic one legged stance.

Not much detail is given on the experimental set up. For this reason the reader cannot determine whether the boundary conditions of the FE model were appropriate. Data was gathered via four rosette strain gages with no description of either the data acquisition or the testing apparatus. Good agreement is claimed between FE and experimental results although one gage location showed tension in the experimental results and compression in the FE results.

Lewis et al. investigated the effectiveness of a collar on a titanium stemmed implant (Lewis et al., 1981). Both FE and experimental procedures were carried out and the results were compared in a qualitative fashion, showing good agreement. Little detail is given on either the experiment or the FE analysis. This study makes its point concerning the effectiveness of collars, but it was evidently not the intention of Lewis et al. to present this work as a validation of the FE method.

As mentioned earlier, Lotz et al. pursued research directed towards fracture risk assessment. Experimental validation was a part of this research. Two unembalmed human femurs were used. The geometry for the FE model was obtained from CT scans. The mesh was generated using both commercially available image processing software and in-house software. Little technical detail was given.

The FE mesh consisted of 667, 20-noded isoparametric solid elements. Material properties for trabecular bone were assigned based on CT numbers via

$$E = 0.7(CT)^{1.2} \qquad S = 0.003(CT)^{1.4} \qquad \textbf{(2.1)}$$

where E is elastic modulus (MPa) and S is strength (MPa). These relations come from previous work (Lotz et al., 1990). Material properties for the cortical shell are taken from (Lotz et al., 1991b) where longitudinal and circumferential elastic modulus were correlated with CT numbers.

Loads, simulating a one legged stance and a fall were applied to the FE model. Forces were distributed over small areas (three to four elements). To balance the applied loads, all nodes on the most distal face of the cortical shell were fixed. This is not technically correct since there would be strain at this location in the experiment. Prior to testing, each femur was sectioned at mid diaphysis and the distal end embedded in aluminum. Both femurs were tested to failure in a hydraulic materials testing system, one in a one legged stance and the other simulating a fall. Data was gathered via nine rosette strain gages and an Optilog data collection system.

A comparison of FE and experimental results showed significant differences, ranging from 8 to 550 percent. It is suggested that poor strain gage attachment might be a major contributor to this error. The Carter et al., (1977) protocol was used. This might be part of the problem but it also appears that boundary conditions were not given enough

consideration. First, as mentioned earlier, fixing nodes on the distal end of the cortical shell is not valid. Secondly, displacement instead of force would more accurately represent the applied load. This is because the elements over which the load is applied have different elastic modulus, and will deform differently, depending on assigned modulus. In the experiment the loading platen would cause a controlled displacement in all nodes over the contact area. Boundary conditions need to be thought through very carefully in such studies.

2.4 Material Properties

As is already evident material properties are an important consideration in FE studies. In this respect researchers are concerned with what may be considered two distinct types of bone. There is some controversy on this point. The classification is based on porosity, with the material matrix itself being very similar. Compact bone has a porosity between 5 and 30 percent and trabecular bone 30 to 90 percent. Some researchers regard compact and trabecular bone as different materials in an engineering sense (Evans 1973; Pugh et al., 1973). Other authors consider these types of bone to be opposing end of a mechanical-morphological continuum characterized by varying porosity and apparent density (McElhaney et al., 1970; Carter et al., 1977; Martin et al., 1984). In a FE study each element is usually considered to consist of either compact bone, trabecular bone, or implant material. The researcher must assign material properties based on some

measurable quantity, usually density. Most recently, CT data has been used to obtain measures of density without actually sectioning the sample. The material properties of bone are covered quite extensively in the literature. Because the present author's focus is on assigning material properties based on density measurements, only papers that deal specifically with this issue will be discussed. For a more complete review on the material properties of bone the reader should consult Keaveny et al., (1993) who published an excellent review on the material properties of trabecular bone and Lee (1995) who reviewed work on both trabecular and cortical bone. What follows is a brief review of bone as a material and specifically how elastic modulus relates to bone density.

Carter et al. published what has become the most referenced relationship between density and elastic modulus (Carter et al., 1976). Carter et al. worked under the assumption that the microscopic material properties of compact and trabecular bone are similar. The trabecular bone is similar in structure to open celled rigid plastic foams or porous concretes. In these materials apparent density (dry weight divided by bulk volume) is the most important predictor of material properties. Carter et al. mechanically tested 100 cylindrical sections of human trabecular bone. Strain rates ranged from .001 to 10. Load deformation curves were plotted for each specimen and the elastic modulus determined from the slope of the linear portion. Using a power law relationship similar to that used for plastic foams Carter et al. arrived at:

$$E = E_c \left(\frac{d\epsilon}{dt}\right)^{0.06} \left(\frac{\rho}{\rho_c}\right)^3 \quad \textbf{(2.2)}$$

E is the elastic modulus of bone, E_c is the measured elastic modulus of cortical bone , $d\epsilon/dt$ is the strain rate, ρ is the apparent density of bone, and ρ_c is the density of cortical bone. Human cortical bone tested at a strain rate of 1.0 s^{-1} has a compressive modulus of $2.21 * 10^4$ MPa. Assuming that cortical bone has an apparent density of 1.8 g/cm^3 then:

$$E = 3790 \left(\frac{d\epsilon}{dt}\right)^{0.06} \rho^3 \quad \textbf{(2.3)}$$

Now E must be in MPa and ρ in g/cm^3. This relationship (Equation 2.3) has been used and referenced widely in FE studies of the human femur and has been applied to both cortical and trabecular bone (Keyak et al., 1993; Rohlmann et al., 1983; Keaveny et al., 1993; Keaveny et al., 1994; Edidin et al., 1991; Bartel et al,.1990). Recently developed bone remodelling algorithms also use the Carter and Hayes relationship (Skinner et al., 1994; Huishes et al., 1992; Carter et al., 1989; Beaupre et al., 1990; Fyhrie et al., 1990; Van Rietbergen et al., 1993).

Schaffler et al. set out to determine if it is reasonable to treat compact and trabecular bone as a single structural material, differing in mechanical properties, only through variation in porosity (Schaffler et al., 1988). Mechanical testing was carried out on fresh femoral and tibial diaphyses of steers. It is argued that the mechanical properties of bone in steers

and humans is very similar. Carter et al. had worked with combinations of bovine and human specimens and this assumption was supported. Schaffler, through regression analysis arrived at the following relationship.

$$E = 0.09\ \rho^{7.4} \tag{2.4}$$

Here E represents elastic modulus in MPa and ρ is apparent density in g/cm^3. This equation is for compact bone and takes no account of strain rate. Schaffler et al. claim to have observed no variation in stiffness due to strain rate in their experiments (strain rates of 0.01 and 0.03). This is not surprising since based on Carter and Hayes there should only be a 6 percent difference for these strain rates. Schaffler et al. conclude that a continuous mathematical function such as the Carter and Hayes relation cannot describe the elastic properties of both trabecular and compact bone. Compact bone stiffness is proportional to apparent density raised to the power 7.4 while trabecular bone stiffness is proportional to apparent density cubed. This data set concludes that small changes in apparent density exert a relatively greater influence on the elastic modulus in compact bone than in trabecular bone. This is quite significant in the FE modelling process.

Rho et al. used an ultrasonic transmission technique to investigate the mechanical properties of both cortical and trabecular bone (Rho et al., 1995). They attempted to provide better data on relationships (between density and elastic modulus) for different bone types as well as account for different directions in the same type of bone (anisotropy). Using ultrasonic techniques allowed for use of smaller specimens with less

complicated shapes. This makes fabrication simpler. Such techniques also allow the measurement of several anisotropic properties from a single specimen. These are significant advantages considering the limited size of bones, inhomogeneity, and anisotropy. Considerable detail is provided on the experimental procedures used as well as statistical methods.

Using linear regression the following relationships were found for cortical bone in the human femur.

$$\begin{aligned} E_1 &= -6.087 + 0.010\rho \\ E_2 &= -4.007 + 0.009\rho \\ E_3 &= -6.142 + 0.014\rho \end{aligned} \qquad \textbf{(2.5)}$$

E_1, E_2, and E_3 are elastic moduli (GPa) in the radial, circumferential and superior-inferior directions respectively. ρ is the apparent density(kg/m^3).

For trabecular bone in the proximal femur it was found that:

$$\begin{aligned} E_1 &= -657 + 3.91\rho \\ E_2 &= -506 + 3.64\rho \\ E_3 &= -331 + 4.56\rho \end{aligned} \qquad \textbf{(2.6)}$$

Here the elastic moduli are in MPa.

And using a power law relationship:

$$E_1 = 0.004\ \rho^{2.01}$$
$$E_2 = 0.01\ \rho^{1.86} \qquad (2.7)$$
$$E_3 = 0.58\ \rho^{1.30}$$

Again, the elastic moduli are in MPa.

Rho et al. also report on the relationship between apparent density and CT number.

$$\rho = 1.31 + 1.067\ CT \qquad (2.8)$$

Details of the scanning procedure are provided in the paper which makes this relationship potentially useful. CT numbers correlated better with trabecular bone density than with cortical bone density. The authors explain that this is due to the narrow range of cortical densities. Also the CT slices were thicker than the actual cortical specimen size.

It is interesting to note that linear relationships best described the elastic properties of cortical bone. This is in contrast to earlier studies. In addition, the predictive power of the linear and power law models for trabecular bone were approximately equal. The power law produced significantly better results at higher and lower densities. This is again in contrast with earlier literature, specifically Carter et al. who reported a density cubed relationship. Rho et al. suggest that the two key assumptions made by Carter et al. were wrong: (1) no difference exists between human and bovine bone, and (2) cortical bone is simply dense trabecular bone

CHAPTER 3

CONSTRUCTION OF FINITE ELEMENT MODELS

3.1 Introduction:

From the literature review it is evident that building a FE model of the human femur is neither simple or routine. Most methods employed are time consuming and tedious with only a few recently developed methods utilizing any degree of automation. There are difficulties associated with accurately representing geometry, material properties and boundary conditions. The construction method described here hopes to build on the best attributes of the varied techniques described in Chapter 2, to put in place the best FE model building technique possible. This goal must be accomplished within the context of available FE software, computing hardware, imaging software and medical imaging

facilities. For the work described here, FE models were constructed of a 17 cm section of a femur shaft, a full intact human femur, as well as 3 cm slice sections cut from the full intact femur.

In St. Johns, Computer Tomography (CT) scanners are available at both the General Hospital and St. Clares Mercy Hospital. Both have Toshiba Xpress/SX Flatbed scanners that were utilized, with the cooperation of the hospital technologist, to provide the CT scans used for the construction of FE models.

At Memorial's Engineering two FE software packages (ANSYS and ABAQUS) are available . Both are well established and respected programs but ANSYS (Ansys, Inc., ©1996 SAS IP, Inc., V5.3) was used for this research because of the solid modelling facility that is a part of the existing package. This solid modeller was an integral part of the modelling techniques developed for this project. If ABAQUS (©1997 Hibbitt, Karlsson and Sorensen, Inc.,V5.7) had been used a stand alone solid modeller would have been required and it was feared there may have been incompatibility problems to overcome.

Specialized software is needed to simply view and manipulate CT scans. Both ImageTool (ImageTool for Windows V1.28, ©The University of Texas Health Science Centre in San Antonio) and OSIRUS (Medical Imaging Software V3.12, a package from The University Hospital of Geneva, available from the Internet) were down loaded free of

charge from the Internet and proved adequate for these purposes. Other required software has been developed in-house for the specific needs of this project and the linking together of the previously described resources.

3.2 Constructing a 17 cm Femur Shaft Section:

The purpose of modelling the 17 cm femur shaft section was to provide some preliminary experience and results to guide the modelling of the full femur. Various techniques were tried and compared using this simpler geometry. A decision was made to use solid modelling techniques as opposed to direct mesh generation, based upon experience gained in this modelling process. Methods that involved direct mesh generation were extremely tedious and showed little potential for automation. The following paragraph describes a modelling procedure that resulted from some trial and error. Figure 3.1 depicts the 17 cm femur shaft section as it was mechanically tested, mounted between two parallel faced load platens.

The 17 cm shaft section was CT scanned at 0.5 cm intervals. The scan slices were perpendicular to the experimental loading axis defined in Chapter 4. This significantly simplifies the application of loads to the FE model. This orientation was achieved by scanning with one load platen still in place. A simple carpenter's square was used to ensure that the end platen was perpendicular to the scanner bed while the load axis was

lined up with the scanner axis. The resulting CT data set consisted of 35 separate digital images (512 by 512 pixels), each corresponding to a slice plane that intersects the load axis at 90 degrees. Each pixel value (CT number) provides both geometric and material property information.

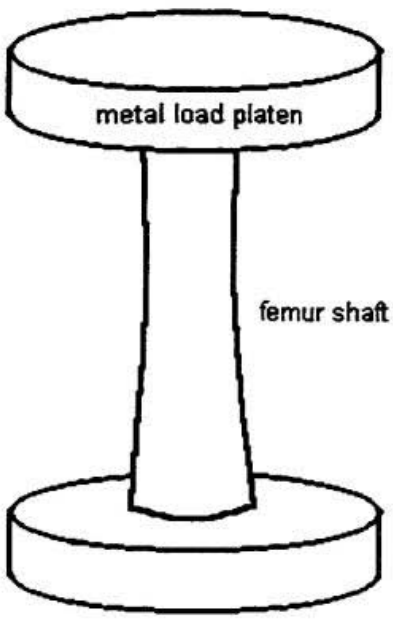

Figure 3.1 - 17 cm femur shaft section mounted between two metal load platens.

ImageTool, a medical imaging software package, was used to both view and analyse CT data. A tool is available within ImageTool that allows the user to place points at any desired location within the image and subsequently save the spatial coordinates of these points in ASCII txt format. This facility was used to place 16 keypoints around the outside of each slice of the 17 cm femur shaft section. In addition 8 keypoints were placed around the inside edge. These keypoint sets were used respectively to define the

outside and inside surfaces of the femur shaft (a femur shaft is hollow). Figure 3.2 illustrates the placement of these points on a CT slice 30 mm from the proximal end of the specimen. The resulting set of keypoints (24 per image slice) were used to construct a solid model in ANSYS. This was accomplished using the splining and skinning capabilities available within the ANSYS solid modelling module.

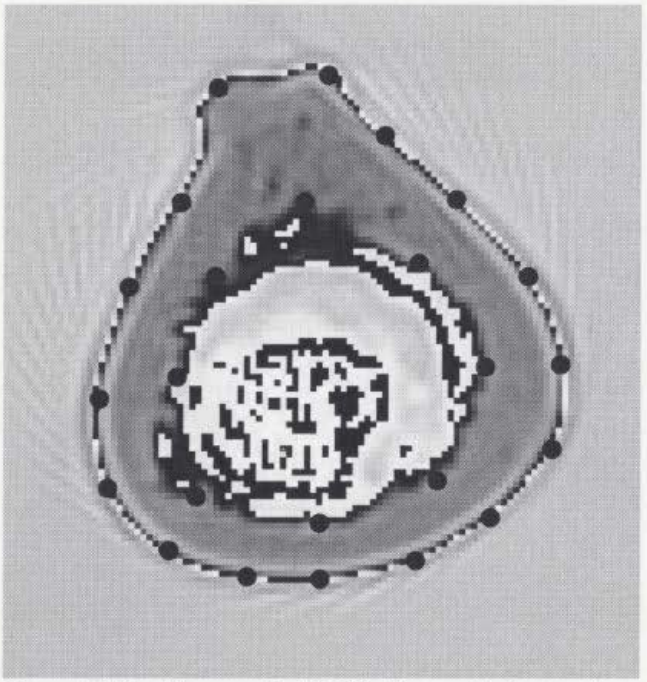

Figure 3.2 - Femur shaft CT slice with keypoints placed around inside and outside edges.

Once the solid model is complete it can be converted directly to a FE model, again within the ANSYS preprocessor. This process essentially involves meshing the solid model with a suitable element type from the ANSYS element library. The element chosen was the "SOLID92", a 3-D 10- noded tetrahedral solid. The element has a quadratic displacement behaviour and is well suited to model irregular shapes such as

human bones. It is defined by ten nodes each having three degrees of freedom: translations in the x, y, and z directions. Meshing a solid model with quadrilateral elements (ie. bricks) such as "Solid95" is only possible with very simple geometries. Using bricks would require direct mesh generation. The resulting FE model contained 1442 elements and is depicted in Figure 3.3.

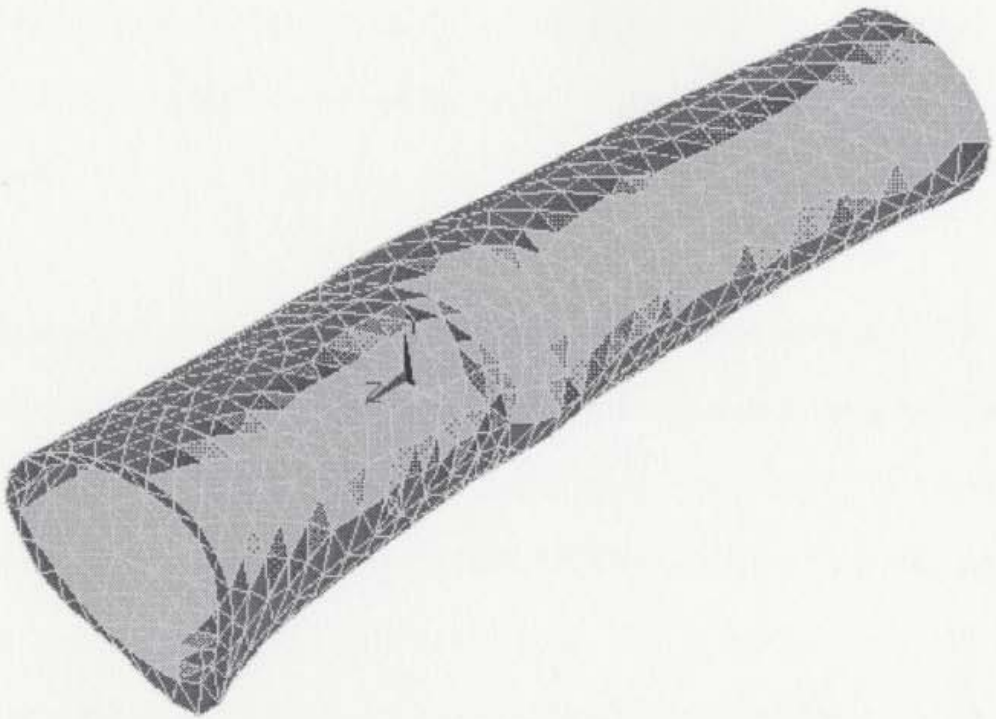

Figure 3.3 - ANSYS plot of 17 cm femur shaft section.

Bone is an inhomogeneous material which means that its material properties vary spatially. The CT data, with a spatial resolution of 0.35 mm in each slice, may be used to assign material properties to the FE model. Each CT slice is a 512 by 512 matrix of CT

numbers that are indirectly related to bone elastic modulus via bone density. The CT numbers are in Hounsfield units where air (non bone) has a value of -1000 and water has a value of 0. Cortical bone in this specimen has an average value of 1800. This was determined by carrying out some statistical work within ImageTool. Bone density may be estimated from CT numbers by simple linear interpolation, utilizing non bone and cortical bone as reference points. Bone density in turn may be used to predict elastic modulus. Various researchers such as Carter et al., (1976) and Rho et al., (1995) have published relationships between elastic modulus and bone density. Carter's is the most widely referenced and simplest and was used for this preliminary study (17 cm shaft section).

To make practical use of CT numbers in assigning material properties to individual elements, a link is needed between the CT data and the FE model. In-house software and techniques were developed that accomplishes this goal in three stages. First, each element centroid location is exported from ANSYS and written to a file. Secondly, this file is read, along with the CT data file and held in memory simultaneously. Some preprocessing of the CT data is necessary to reduce file sizes and memory requirements. From these two files each element is assigned a CT number. Thirdly, elastic moduli are assigned as a function of CT numbers to each element in the FE model. In the resulting model a unique modulus is assigned to each element, so that the inhomogeneous nature of human bone is represented.

Finite Element loads and boundary conditions must be applied in a fashion that accurately reflects the actual loads and boundary conditions present in the mechanical tests (detailed in Chapter 4). For this test (17 cm femur section) the bone was axially loaded between two metal platens. Because the platens were much stiffer than the bone, the experiment is simple to model. All nodes at the distal end were fixed while a displacement load was applied to each node at the proximal end. The magnitude of the displacement was such that an overall load is produced that matched the experimental load of 100 kg. This was easily achieved by applying an arbitrary displacement load, calculating the total reaction force, and then scaling the displacement to produce the desired overall load. This method is appropriate only in a linear model.

The model was solved and calculated strains were exported to a table for locations where strain gages were attached during mechanical testing. FE strains were ultimately compared to experimental strains for verification.

3.3 Construction of the Full Intact Femur:

The process used to model the whole femur was somewhat similar to that used to model the 17 cm femur shaft section. Significant differences occurred in (1) CT scanning technique, (2) the method of keypoint extraction from the CT data, and (3) application of loads and boundary conditions.

The loading axis for the full femur was significantly more difficult to define. It is desirable to test the femur in an orientation that is physiologically relevant. This has not been the case with most FE work in this area. The problem with using physiological boundary conditions is that they are complex and more difficult to model. Experimental tests must be reproducible and provide boundary conditions that can be modelled accurately. With these criteria in mind an attempt was made to model and test the full femur in an orientation and configuration that reflects physiological conditions, while allowing reproducibility and ease of modelling. The load axis was defined as a line extending from the highest point on the ball shaped head of the femur to the midpoint of a segment connecting the centroids of the condyles (Figure 3.4).

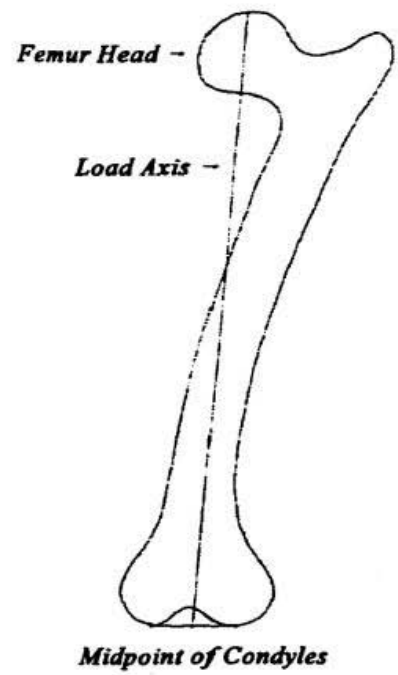

Figure 3.4 - Schematic of the full femur load axis, extending from highest point on the head to midpoint of segment connecting condyle centroids.

Again the specimen was CT scanned in an orientation that positions the scan slices perpendicular to the load axis, and again this simplifies application of boundary conditions. This was achieved by scanning, with the femur positioned between its load platens. This insures that the load axis is parallel to the scanner bed which positions the scan slices perpendicular to the load axis. The design of the load platens, detailed in Chapter 4, renders this process extremely simple. The platens are moulded in a fashion that sets the load axis of the femur parallel to the lateral sides of the platens. When the femur is mounted between the platens and laid on a flat surface (scanner bed) the load axis of the femur will be parallel to that surface. Figure 3.5 shows the femur in the scanning orientation, held between its custom made load platens.

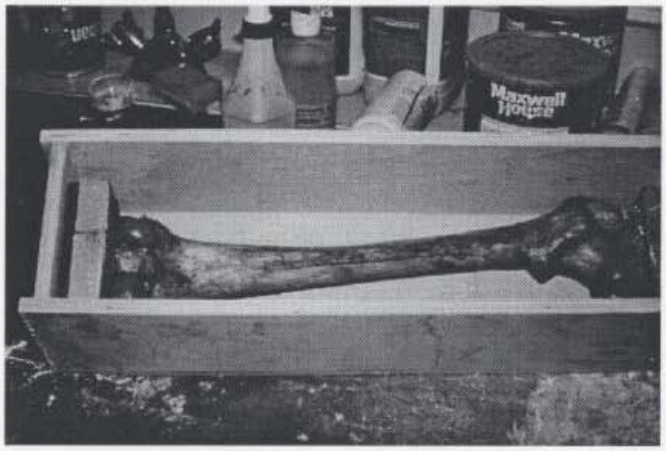

Figure 3.5 - Femur held in scanning orientation between custom made load platens. The purpose of the plywood box is to embed the femur in plaster for subsequent sectioning.

The geometry of the femur head is significantly more complex than the femur shaft. Initial attempts to model geometry by manual keypoint extraction proved difficult for two reasons. First, the process was extremely time consuming. More keypoints were needed to accurately depict the complex geometry of the femur head, and their manual placement proved extremely tedious and time consuming. Secondly, when placing keypoints manually it is difficult to properly align them in adjacent slices (longitudinal alignment). This was manageable in the shaft section with only 16 points and a relatively simple geometry but with the full femur it was impossible. Non-alignment causes large geometric gradients or "rumples" in the surface of the solid model. These in turn produce meshing problems due to excessive element distortion and aspect ratio. The problem was addressed by developing software that could automatically place and extract keypoints from the CT data.

Edge detection techniques are well established and are gaining wide application in the image processing field. In-house software was developed by Dawna Greening that locates the outside and inside edges of the femur in each CT slice, and places equally spaced keypoints along each edge (see Appendix A for details). The keypoints are then written to a file in a format that is readable by ANSYS. The solid model is then constructed in ANSYS using the same process as before. This technique eliminates rumples while automating what was a tedious and time consuming process.

FE models of this magnitude (greater than 5,000 elements) require significant computer

resources. However, the educational version of ANSYS allows no more that 10,000 nodes. As we were concerned primarily with calculating strains in the proximal region of the femur, it was decided to model only a proximal portion of the femur, but simulate a full femur test by appropriate application of boundary conditions. Two full femur models were generated. The first consisted of 4345 elements (7780 nodes) and extended from the femur ball ($z = 0$) to a point on the shaft 30 cm below. The second consisted of 7294 elements and extended from $z = 0$ to $z = 10$ cm. Mesh sizes for these models were 7 mm and 4.5 mm respectively. Both models are shown in Figures 3.6 and 3.7.

Experimentally, the femur was restrained at the head by a custom made metal platen (proximal), dimpled to fit the actual femur head. Load was applied via a custom made metal platen (distal) fitted to the condyles in a fashion similar to the configuration in the actual knee joint. The proximal platen was modelled and attached to the femur model, within ANSYS. The platen being geometrically simple was modelled using graphic primitives. The platen was then fixed at a point where its upward facing surface intersects the loading axis. The modelled platen was free to rotate about this point. This is because the femur head was free to rotate within its dimple during the mechanical test. To the distal end of the model, a virtual platen was attached and load was applied at the point where the platen intersects the load axis. This loading technique generates bending moments equal to those in the actual mechanical test without having to model the whole femur and actual distal load platen.

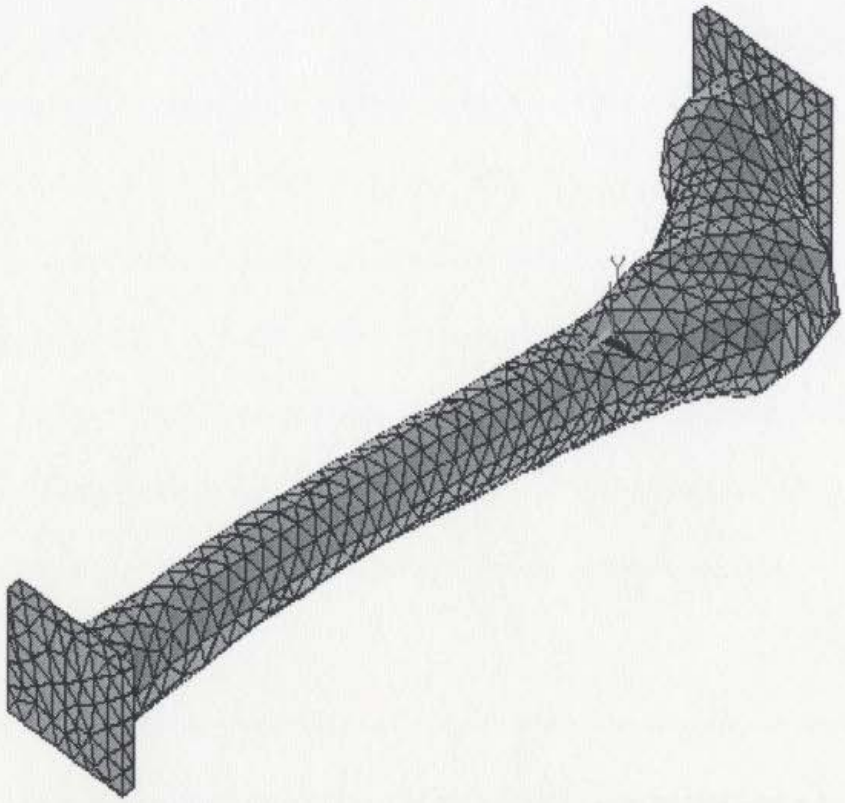

Figure 3.6 - FE model of full femur using a 7.0 mm mesh.

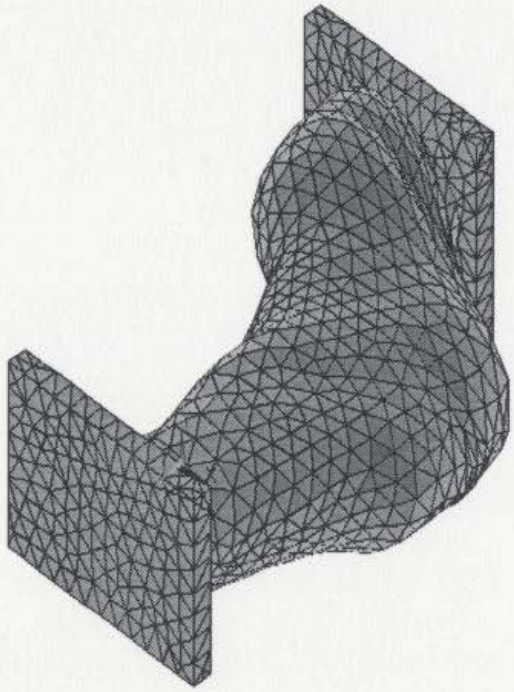

Figure 3.7 - FE model of full femur using 4.5 mm mesh.

Material properties were assigned to the full femur model using the same process outlined for the 17 cm shaft section. The only difference is in the assignment criteria. The relationship between elastic modulus and density was not simply taken from the literature but was modified to reflect the uniqueness of the femur being tested. This modification was based on data gathered from mechanically testing and modelling 3 cm femur slice sections as described in the following section. These slice sections were cut from the full intact femur presently being discussed, after the tests described here.

After assignment of material properties, and application of boundary conditions the model was complete and could be solved within ANSYS. Subsequent to this, stress/strain data for any point within the model was available. Strain data was exported into tables for locations where gages were attached on the actual femur during mechanical testing.

3.4 Modelling Femur Slice Sections:

In all, six femur slice sections were modelled, each corresponding to an actual slice section physically cut from the real femur. Sections were labelled T7_B10, T10_B13, T13_B16, T16_B19, T19_B22, and T22_B25. "T" refers to top or end of the section towards the proximal end of the femur while "B" refers to bottom or the distal end. The

numbers are distances along the load axis in cm, and are referenced from the point where the load axis exits the femur head. Figure 3.8 depicts a typical slice section. The actual cutting process is described in Chapter 4. These models were created using the same technique already employed with the full femur. The only significant difference is that the boundary conditions are much simpler. All nodes at one end were fixed and a z direction displacement was applied to all nodes at the other end. This simulated the test configuration detailed in Chapter 4, where the slice specimen was axially loaded between two metal plates.

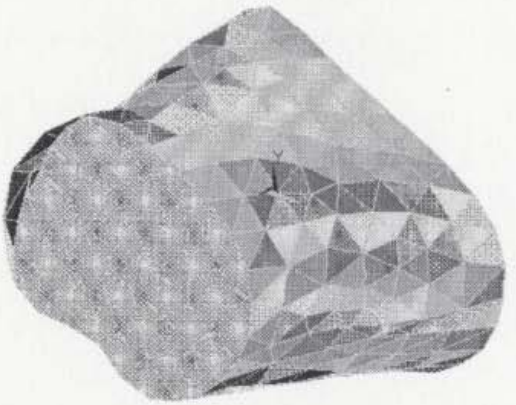

Figure 3.8 - FE model of slice section T7_B10.

The main purpose of modelling and testing these slices was to learn more about the material properties of this particular human femur. Data gathered from this work may be used in assigning material properties to the full intact femur model. The actual sections corresponding to these models were all mechanically tested and experimental strain data

is available for comparison with FE strains. Since the geometry is relatively simple and the material properties less variable than in the full femur, these models can be used to investigate published relationships between bone density and elastic modulus. Since there is significant variation from one femur to another it is necessary to validate or calibrate these published relationships to account for the uniqueness of the specific femur used in this research. Essentially, the material property assignment criteria are altered to achieve the best possible fit between FE strains and experimental strains. This is justified within the context of a simple geometry and simple boundary conditions. The technique also has the advantage of being able to obtain material property data without having to machine the specimens to perfect cylinders or cubes as is the case with typical or conventional material property work.

CHAPTER 4

A DESCRIPTION OF EXPERIMENTAL VERIFICATION

4.1 Introduction:

As was previously discussed, experimental verification of FE calculations are essential to this project. FE models were constructed for (1) a 17 cm section of human femur shaft, (2) a full intact human femur, and (3) a total of six, 3.0 cm slice sections cut from the full intact femur. Experiments were designed and carried out to verify FE results for all three cases.

4.2 Environmental Control:

Subsequent to some initial testing it was realized that the material properties of bone are quite sensitive to environmental conditions (ie. water content). Bone looses or gains water until it reaches a stable equilibrium with its environment. If experimental data is gathered under arbitrary environmental conditions then cross referencing of data sets is meaningless. Material properties determined from experimental data are useless unless the environmental conditions are known and can be duplicated in other mechanical tests. For these reasons it was decided to design, construct and utilize an environmental control system.

There are actually two separate stages of environmental control: (1) Since biomaterials take a finite amount of time to reach equilibrium with their surroundings, preconditioning of the bone prior to testing is necessary. Due to storage requirements for biomaterials this process must be carried out in a cooler at approximately 5^0 C. (2) Humidity must be controlled during actual testing. Ideally a specimen would be at equilibrium during a test (ie. no exchange of water with the surroundings). This may not be possible in practice but exchange was kept to a minimum and each test was performed under the same conditions.

Eliminating any exchange of moisture during testing is made difficult by the necessity of

storing specimens at 5^0 C while testing them at room temperature. Relative humidity, which is rather straightforward to control, is defined as the amount of water vapour in the air relative to the maximum amount that can be held at that particular temperature. The critical factor that determines moisture exchange with biomaterials is partial pressure of water vapour and not relative humidity. The relationship between partial pressure and relative humidity is:

$$P = \frac{RH}{100} * P_o \qquad (4.1)$$

where: P = partial pressure

RH = relative humidity

P_0 = partial pressure of pure water at temperature T

Even if a stable relative humidity is maintained over the temperature range (5 to 25 ^{0}C) the vapour pressures would be significantly different due to the different values of P_0 (ie. 0.87 kPa @ 5^0C and 3.17 kPa @ 25^0C). For this reason it is not practical to test and precondition at equal vapour pressures. Relative humidity was controlled in both processes in a consistent fashion from test to test and a simple experiment was conducted to determine the rate of moisture loss from specimens during tests.

Relative humidity is quite simple to control. The relative humidity above pure water in a closed system is 100%. At 5^0C this provides a partial water vapour pressure of 0.87 kPa for bone preconditioning. Specimens were stored above water in a closed container for a

period of time adequate to allow attainment of equilibrium between the bone and its surroundings. During testing a containment system housed the specimen, into which 75% humidity was be circulated. 75% air was provided by bubbling air through a saturated sodium chloride solution.

The details of this 75% humidity source are provided in Appendix B. Air at 75% humidity and 25^{0}C provides a vapour pressure of 2.376 kPa.

After three days of preconditioning (100% humidity and 5^{0}C) and subsequent storage (75% humidity and 25^{0}C) above a sodium chloride solution, the rate of mass change in specimens was quite small (less than 0.1% per hour). Since tests are typically under one hour duration (including setup) this procedure ensures reasonable consistency.

4.3 Mechanical Testing of a 17 cm Section of Femur Shaft:

In this section a 17 cm section of human femur was mechanically tested in compression for validation of FE calculations carried out on the same bone specimen. Prior to testing the specimen was mounted between two parallel faced Cerobend™ platens (Figure 3.1). Cerobend™ is a low melting point (158^{0}F) lead, tin, bismuth, and cadmium alloy suitable for the mounting of biomaterials (supplied by Canada Metal Company, Montreal, Canada) . The ends of the specimen were placed in liquid Cerobend™ and the alloy was allowed to harden thus encapsulating the specimen to a depth of approximately 2.0 cm.

Care was taken to ensure that the faces of the platens were parallel, with the specimen aligned in the orientation desired for testing (ie. load platen faces perpendicular to load axis). This orientation matches the loads applied in the FE model discussed in Chapter 3. Non-parallel platen faces would introduce unwanted bending moments not accounted for in the FE model.

Next, three rosette strain gages (120 ohms) were attached at equal angular distances around the lateral surface of the bone, 8.0 cm from the proximal end. Appendix C details the strain gage attachment procedure. The whole configuration (specimen, platens, and strain gages) was mounted in an Instron Model 123 test frame and loaded in stroke control at 0.50 mm/min. The crosshead was manually stopped when the load reached 200 kg. Data was acquired at 1.0 Hz using Labtech Notebook software, a DAS 20 A/D card and a EXP-GP multi-plexing signal conditioning board. Raw data files were written in ASCII text format and subsequently imported into Corel Quatro Pro for visualization and further processing.

4.4 Mechanical Testing of a Full Intact Human Femur:

It is desirable that mechanical tests as well as FE models simulate physiological conditions. It is also important that experimental boundary conditions be well defined and reproducible. Most importantly for present purposes, boundary conditions in mechanical tests must be expressible in FE terms. A compromise must be found between these sometimes conflicting goals. Typically, researchers have sectioned the femur someplace above the condyles and have potted the femur in either metal, fibreglass, or epoxy resin. See Chapter 2 for details. This ensures reproducibility, but experimental loads will differ significantly from physiological loads. There is also some question about the validity of the manner in which this restraint has been typically represented in FE models. A full displacement restraint is commonplace but this is not entirely correct since there may be substantial strain in the femur shaft where the shaft enters the pot.

To ensure reproducibility while maintaining a reasonable resemblance to physiological conditions a fresh approach was taken. First of all, the femur was not sectioned or altered in any way. The loading axis was defined as an imaginary line connecting the upper most point on the femur head with the midpoint between the centroids of the two condyles (Figure 3.4). Now that the loading axis is defined, a procedure must be developed to accurately mount the specimen in this orientation.

The femur was not potted or embedded but held securely within dimples moulded into

rectangular Cerobend™ platens, using the femur itself to form the dimple as liquid Cerobend™ solidified around it. A latex surgical glove served as a barrier between the metal and the bone. It was critical in this moulding process that the femur be held securely with the load axis vertical. This was accomplished with simple laboratory stands, clamps, and a carpenter's plumbline. Once the femur was in position liquid Cerobend™ was poured into a plastic mould, positioned appropriately so that a dimple would be formed in the platen's upper surface by the femur ball, with the femur secured in the actual load orientation. This process forms the proximal load platen. The process was then repeated with the femur in the opposite orientation thus forming a distal platen custom fitted to the femur condyles. The resulting Cerobend™ platens were drilled and a steel plate attached to each one on the side opposite the dimpled surface. These plates provide a means of attachment to the load frame. Alignment of the load platens is now sufficient to ensure that the femur is loaded along the mechanical axis as previously defined. The platen may also be used to ensure that the femur is in the proper orientation for CT scanning and physical sectioning. This is significant since it is desirable to both scan and section perpendicular to the load axis. Finally the platens were attached to the MTS Model 312.21 test frame via some simple in-house designed and fabricated parts. Care was taken to ensure alignment of the platens with each other, and with the load axis of the test frame. Figure 4.1 shows the femur securely held between the platens in the test frame. A ball bearing was installed underneath the distal platen (between two steel plates) to eliminate any unwanted bending moments.

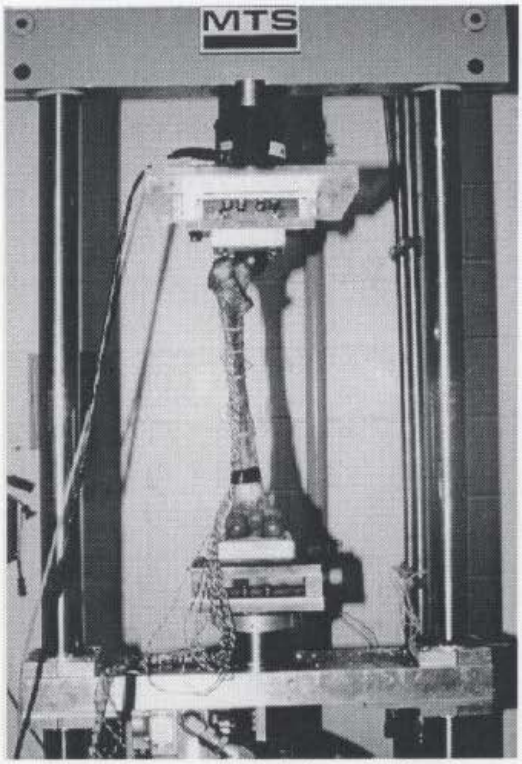

Figure 4.1 - Femur held securely between its load platens in the MTS test frame.

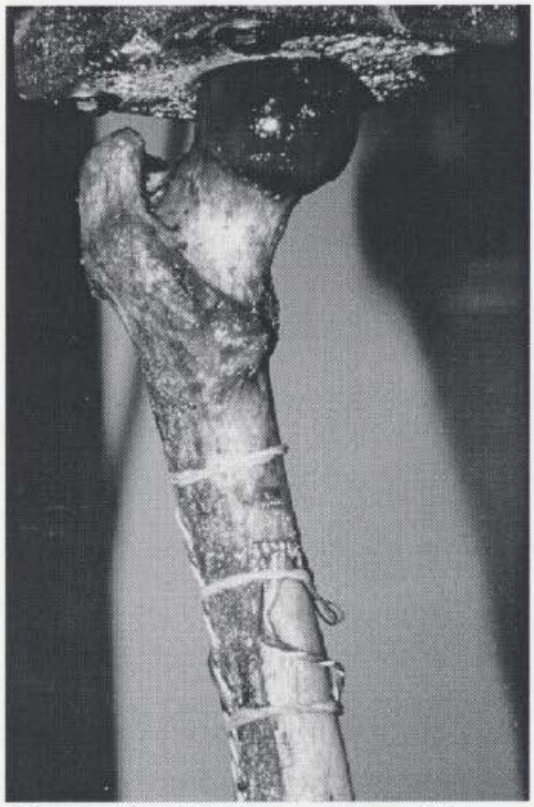

Figure 4.2 - Proximal portion of femur and load platen pictured during a mechanical test.

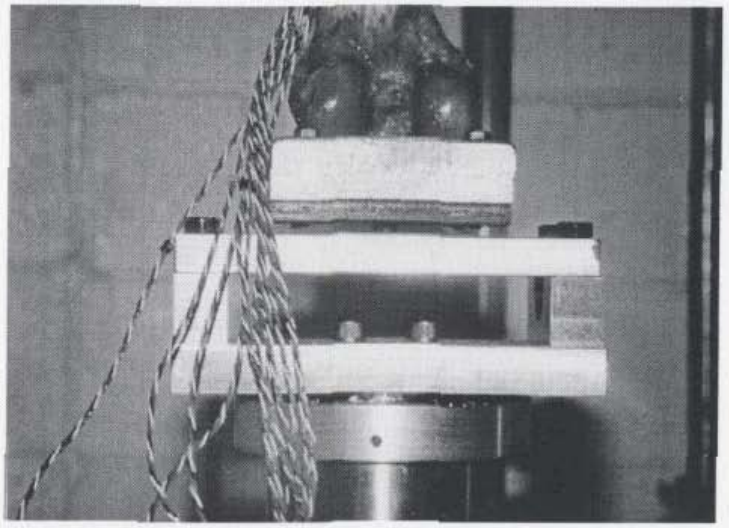

Figure 4.3 - Distal portion of femur and load platen pictured during mechanical test.

The proximal and distal portions of the femur along with corresponding load platens is pictured in Figures 4.2 and 4.3 respectively.

Loads were applied in load control utilizing the MTS test frame, a hydraulic actuator, a MTS Model 407 controller, and Labtech Notebook software. An external analog load function was provided to the controller via Labtech Notebook. A digital file (ASCII txt) was constructed which Labtech converted to the appropriate analog signal. The actual load consisted of five ten second 14 kg ramps, up to a maximum load of 70 kg. Each ramp ended with a 30 second relaxation period, allowing viscoelastic effects to subside. The load was removed in a similar fashion with five -14 kg ramps down to 0 kg. The 30 second relaxation (actually recovery) period was also included in the removal of load. The overall loading sequence was repeated twice for each test for a total test time of approximately 15 minutes. In between sequences the load was cycled from minimum to

maximum and back to minimum 5 times using a 15 second ramp. Figure 4.4 depicts the application of load and a typical strain response.

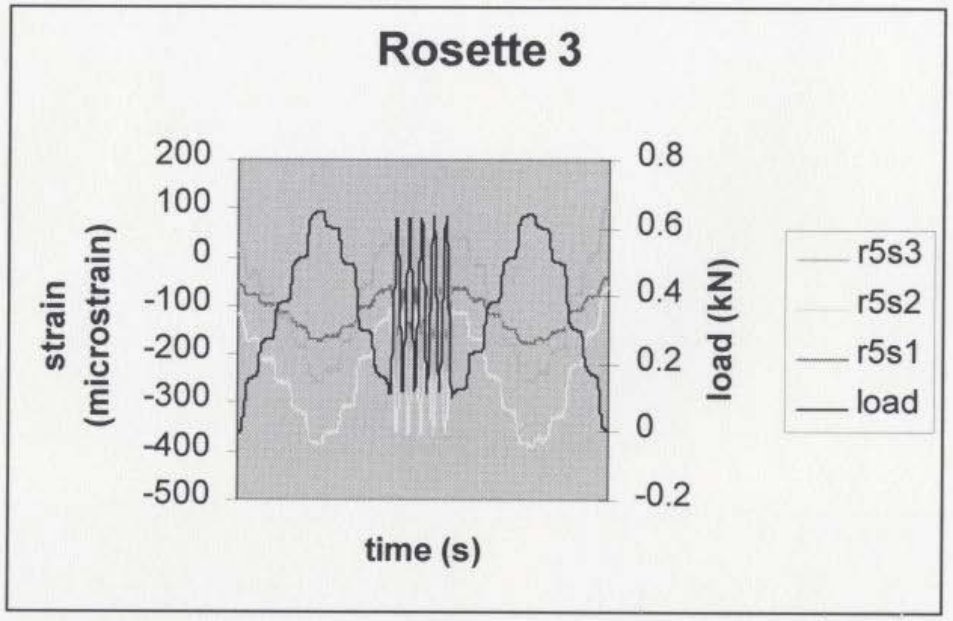

Figure 4.4 - Application of load to the full femur along with a typical strain response.

Seven rosette strain gages were attached to the lateral surface of the femur at carefully recorded and strategic locations so that measured strains could be compared with those calculated by FE. Figure 4.5 shows the femur in four orientations with the strain gages clearly visible. Details of strain gage attachment are outlined in Appendix C. Data was acquired at 1 Hz using Labtech Notebook software, a DAS 20 A/D card and a EXP-GP multi-plexing signal conditioning board. Raw data files were written in ASCII txt format and subsequently imported into Corel Quatro Pro for visualization and further processing. Principle strains were calculated from rosette data for comparison with FE results.

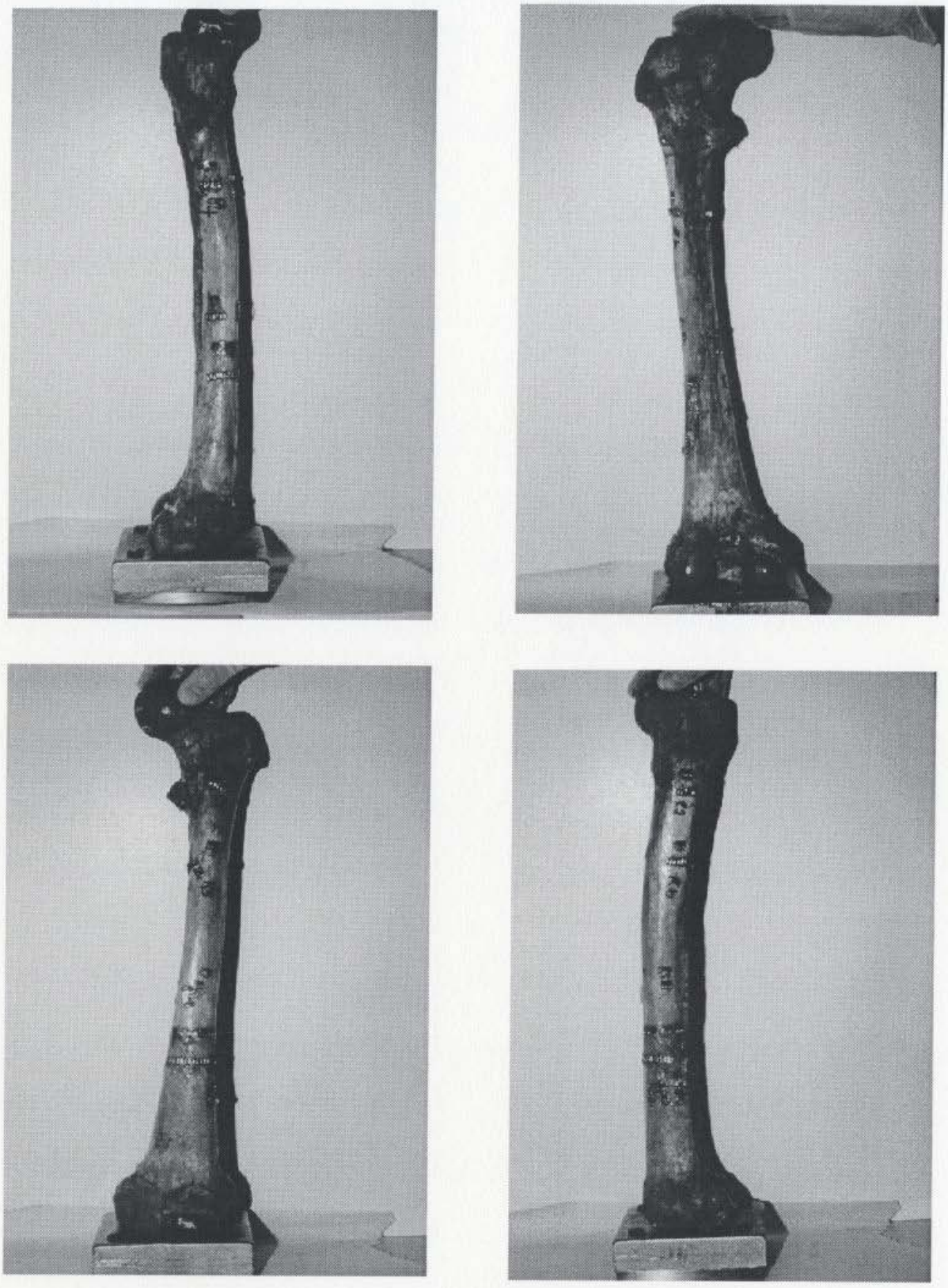

Figure 4.5 - Femur shown in four orientations with strain gages attached.

4.5 Mechanical Testing of Femur Slice Sections:

A common method of obtaining elastic moduli is to section small cubes from the bone and measure stress and strain directly under compression in a standard test frame (Carter et al., 1976, and Schaffler et al., 1988). However, even with edges as small as 5 mm cubes cut from many parts of a femur will not be uniform in structure or density, and it is impractical, if not impossible, to cut such cubes from many portions of the bone, including the outer layers of cortical bone. Similarly, tensile test specimens may be cut longitudinally from the shaft of a femur, but not readily from the head.

It was therefore decided to test in compression complete slices of a femur, with parallel ends parallel to CT scan slices, and produce a FE model slice (which can be done with smaller elements than used for a model of the whole femur). The object is to find the relationship between CT numbers and modulus which will cause the load deformation relationships of the slice to match that observed in a mechanical test of the slice. Of course a Poisson's ratio must also be assumed in the models. The hypothesis was that by taking advantage of the ability to model the constraints at the test platen - bone interface, as well as the deformation and the stress/strain distribution in the bone, it will be possible to identify or devise a CT number - modulus relationship which works with the individual slices and that this relationship will also be valid for the whole femur, and the femur with an implant. This approach should be as good as the testing of small cubes, or the like, for

the determination of mechanical properties of the bone. This technique does not appear to have been used before. In this work we are modelling human cadaver bone which has been preserved for some time. If successful with bone in this state, the work should be extended to fresh bone.

The first step was the physical sectioning of the femur at predetermined locations. There does not seem to be any previous publication that details this process. The femur was sectioned in planes perpendicular to the loading axis at 3.0 cm intervals starting 7.0 cm from the highest point on the femur head. The practicalities of strain gage attachment eliminated the use of sections less than 7.0 cm from the reference point.

The irregular shape of the femur makes it difficult to continuously hold in any given or well defined orientation while it is being sectioned. The most convenient solution was to embed the whole intact femur into a block of solid material that may be easily cut. It was decided after some experimentation to use Plaster of Paris. Plaster of Paris is readily available, low cost, easy to cut, cures with minimal volume change, and separates from bone easily after the cutting is complete. The femur was held in the proper orientation with its loading platens inside a rectangular mould, into which the Plaster was poured. The Plaster was allowed to cure and the mould removed leaving a rectangular block whose ends are parallel to the desired section planes and lateral sides are parallel to the loading axis. Figures 4.6 and 4.7 illustrate this process.

Figure 4.6 - Femur held in scanning orientation between custom made load platens. The purpose of the plywood box is to embed the femur in plaster for subsequent sectioning.

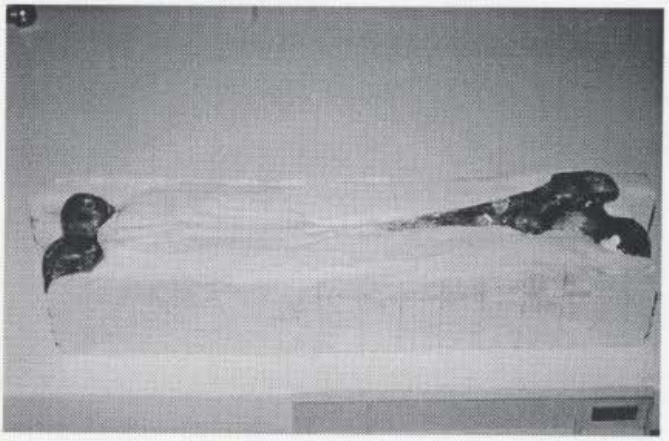

Figure 4.7 - Femur embedded in plaster in scan / load orientation. The sides of the plaster block are parallel to the load axis.

The next step is the actual cutting of the sections. Some simple tests verified that a carpenter's back saw would be adequate to cut both Plaster of Paris and bone. The challenge was to make the cuts perpendicular to the load axis and as planar as possible. An in-house mitre box was designed and fabricated (somewhat similar to a carpenter's mitre box) to facilitate this process. The cutting was carried out and six femur sections were stored for further testing. Figure 4.8 shows the femur being sectioned.

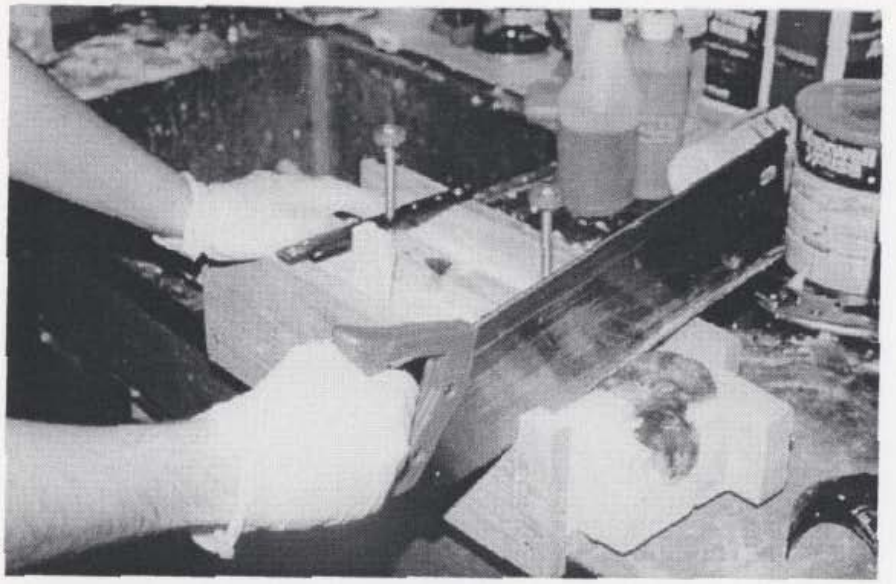

Figure 4.8 - Femur being sectioned using a back saw and an in-house designed mitre box.

The same experimental setup previously used for the full femur test was again utilized. This included load frame, data acquisition system, environmental controls, and loading sequence. The only differences were that one rosette was used instead of seven (except on slice T7_B10 which had two gages attached, subsequently labeled T7_B10_S and T7_B10_B) and different boundary conditions were employed. The sections were simply placed between two flat metal loading platens. The lower platen was again placed on a ball bearing to eliminate bending moments. Figure 4.9 shows a slice section being tested.

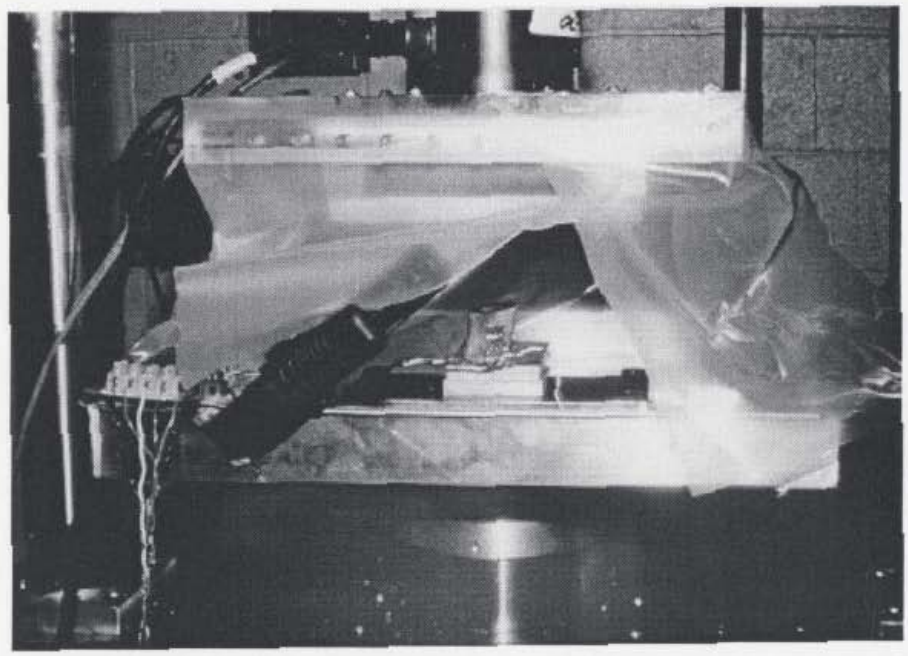

Figure 4.9 - Femur slice being mechanically tested.

CHAPTER 5

COMPARISON OF FINITE ELEMENT RESULTS TO EXPERIMENTAL RESULTS

5.1 Introduction:

The overall goal of this project was to validate finite element calculations for a full intact femur, and to this end experimental and FE results are compared in this chapter. There were however two sets of preliminary results leading up to validation of the full femur model. First, preliminary work was carried out with a 17 cm femur shaft section. These results, presented first, established confidence in the modelling techniques used before

embarking on the construction of a much more complex model (full intact femur). This stage was particularly important, considering that all the modelling techniques were developed in-house with little prior experience. Before material properties were assigned to the full femur model, investigative work was carried out on femur slice sections to gather material property data. This data was subsequently used to select and calibrate criteria for the assignment of material properties to the full femur. These results are presented next. Finally strains calculated in both full intact femur models (7 mm and 4.5 mm meshes) are presented and compared to measured strains.

5.2 Results From 17 cm Femur Shaft Section:

As already described in some detail (Section 4.3), mechanical tests were carried out on a 17 cm section of human femur shaft to verify some preliminary FE results. Strains were measured at midshaft (8.0 cm from the proximal end) and are presented in Table 5.1 along with calculated FE strains. Because this is preliminary work, meant only to instill some confidence in the FE modelling techniques employed, only z-direction strains were calculated. The excellent agreement between FE and experimental results confirm that the modelling techniques employed are valid and may be used to calculate strains in a more complex model. In this model, material properties were assigned based on CT numbers using the Carter-Hayes criteria. No adjustment was made for the specific nature of this particular specimen.

Table 5.1: Experimental and calculated strains ($\mu\epsilon$) for 17 cm femur shaft section (load = 100 kg).

	FE model	Experimental	% difference
rosette #	ϵ_z	ϵ_z	ϵ_z
1	-248	-271	8.49
2	-277	-258	-7.36
3	-241	-262	8.02

5.3 Results From Femur Slice Section Testing:

In this section FE strains and measured strains are compared for six femur sections. These sections were physically cut from the full intact femur, mechanically tested, and modelled as detailed in Section 4.5 and Section 3.4 respectively.

The focus is primarily on the development of criteria to assign material properties to FE models of specific femurs based on the results of section tests. Section test results will guide the subsequent assignment of material properties to the full femur model. Initially, the unaltered Carter Hayes relationship (Equation 2.3), was used to assign a linear elastic modulus to each element in each of the slice section models. This relationship between elastic modulus and density is simply a specific form of the general relation,

$$E = A\rho^n \qquad (5.1)$$

arrived at by statistical analysis of a limited amount of experimental data for both human and bovine bone (Carter et al., 1976). There might indeed be significant variation from one human femur to another. The procedure that follows may be useful for determining any such variation.

Table 5.3.1 shows FE and experimental principle strains (ϵ_1 and ϵ_2), obtained from section models, using the unaltered Carter Hayes, relationship as the assignment criteria. The average percent difference for the first principle strain is -17%. If the coefficient "A" in the assignment criteria is adjusted from 3790 MPa to 3128 MPa (ρ in g/cm^3), the error is lowered to 0.5% (see Table 5.3.2). Physically, the structure has been linearly softened in the model. The technique employed, was to calculate the coefficient necessary to adjust the FE strain to match the experimental strain for each section. The average of these calculated values results in a new coefficient that better reflects the specific bone under study. Adjusting "A" does not significantly alter the standard deviation or spread of the results. Adjusting "A" results in an overall stiffening or softening of the FE model. An improved spread in the percent differences may be achieved by adjusting the power of bone density "n".

Table 5.3.1: Comparison of calculated and experimental strains (in $\mu\epsilon$) for femur slice sections (A=3790 MPa, n=3).

Slice	Finite Element		Experimental		% differences	
	$\epsilon 1$	$\epsilon 2$	$\epsilon 1$	$\epsilon 2$	$\epsilon 1$	$\epsilon 2$
T7_B10_B	-482	157	-419	152	-15	-3.3
T7_B10_S	-241	131	-207	131	-16	0
T10_B13	-156	87.5	-106	87.5	-47	0
T13_B16	-236	75	-217	76.2	-8.8	1.57
T16_B19	-129	41	-113	83	-14	50.6
T19_B22	-147	46	-136	37	-8.1	-24
T22_B25	-174	53	-156	46	-12	-15
average percent difference					-17	1.34
standard deviation					13.5	23.8

Table 5.3.2: Comparison of calculated and experimental strains for femur slice sections (A=3128 MPa, n=3).

Slice	Finite Element		Experimental		% differences	
	$\epsilon 1$	$\epsilon 2$	$\epsilon 1$	$\epsilon 2$	$\epsilon 1$	$\epsilon 2$
T7_B10_B	-457	149	-419	152	-9.1	1.97
T7_B10_S	-203	84	-207	131	1.93	35.9
T10_B13	-138	50	-106	87.5	-30	42.9
T13_B16	-200	64	-217	76.2	7.83	16
T16_B19	-111	35	-113	83	1.77	57.8
T19_B22	-128	40	-136	37	5.88	-8.1
T22_B25	-127	47	-156	46	18.6	-2.2
average percent difference					-0.5	20.6
standard deviation					15.5	25.3

There is no theoretical reason why "n" should exactly equal 3. In fact it would be very surprising if "n" did work out to be an exact integer. There may also be some variation in the optimum value of "n" from one bone specimen to another. It will be useful to experiment with values of "n" other than 3. To do this it is necessary to construct a FE model for each "n" value considered. Fortunately the modelling techniques developed for present purposes allow material properties to be modified with relative ease (about two hours work to modify materials and run the model). The process will become even faster as the software evolves and becomes integrated into a comprehensive package.

FE models were constructed for each slice section using n = 2.5 and n = 3.5 in the material property assignment criteria. Again, "A" was adjusted in each case to get the best fit to experimental data for both values of "n". Table 5.3.3 and Table 5.3.4 give results for n = 2.5 and n = 3.5 respectively. In terms of standard deviation, n = 2.5 gave the best correlation between FE and experimental results. Since standard deviation is the best measure of fit between FE and experimental results,

$$E = 4421\rho^{2.5} \left(\frac{d\epsilon}{dt}\right)^{0.06} \qquad \textbf{(5.2)}$$

will be used as the material property assignment criteria for the full femur model.

Table 5.3.3: Comparison of calculated and experimental strains (in $\mu\epsilon$) for femur slice sections (A=4421 MPa, n=2.5).

Slice	Finite Element		Experimental		% differences	
	$\epsilon 1$	$\epsilon 2$	$\epsilon 1$	$\epsilon 2$	$\epsilon 1$	$\epsilon 2$
T7_B10_B	-413	135	-419	152	1.43	11.2
T7_B10_S	-206	81	-207	131	0.48	38.2
T10_B13	-134	49	-106	87.5	-26	44
T13_B16	-202	65	-217	76.2	6.91	14.7
T16_B19	-110	35	-113	83	2.65	57.8
T19_B22	-126	40	-136	37	7.35	-8.1
T22_B25	-149	45	-156	46	4.49	2.17
average percent difference					-0.4	22.9
standard deviation					11.7	24.1

Table 5.3.4: Comparison of calculated and experimental strains (in $\mu\epsilon$) for femur slice sections (A=2302 MPa, n=3.5).

Slice	Finite Element		Experimental		% differences	
	$\epsilon 1$	$\epsilon 2$	$\epsilon 1$	$\epsilon 2$	$\epsilon 1$	$\epsilon 2$
T7_B10_B	-475	156	-419	152	-13	-2.6
T7_B10_S	-189	81	-207	131	8.7	38.2
T10_B13	-137	49	-106	87.5	-29	44
T13_B16	-189	61	-217	76.2	12.9	19.9
T16_B19	-107	34	-113	83	5.31	59
T19_B22	-125	38	-136	37	8.09	-2.7
T22_B25	-151	46	-156	46	3.21	0
average percent difference					-0.6	22.3
standard deviation					15.2	25.2

In the previous discussion the strain rate term was not taken into account. The reader will note that the dependence on strain rate is to the power 0.06 which is quite weak. Also while strain rate can be controlled for simple section tests, it is impossible to control strain rate in a full femur test. Strain rate will vary with location in the full femur as load is applied. In the section tests the local strain rates would be approximately equal to the overall strain rate which can be calculated from crosshead speed but no such relationship exists for the full femur test. For these reasons the strain rate term was set to 1.

It is clear that material property assignment needs further consideration. These results are based on a small number of both mechanical tests and FE models from only one femur. The present work, does however lay the groundwork for future studies. More femurs and sections of the same need to be both mechanically tested and modelled to establish the credibility of this procedure. With more femurs the process can be applied to a wider range of bone structure and properties. In addition, investigating a broader range of "n" values would serve to establish a general relationship between "n" and the fit of FE to experimental results. Further improvements in modelling (ie speed of construction, assignment of material properties, and actual processing) will facilitate this sort of investigation. With our present technology doing calculations for one "n" value with just one slice section takes a significant amount of both human and computer resources.

It is possible to carry out a material property investigation using assignment criteria other than Carter and Hayes as the starting point. A recent publication by (Rho et al., 1995) suggests that human bone may be modelled as a linear function of density as long as trabecular and cortical bone are treated separately. This work also investigates bone's anisotropic nature. Material property assignment criteria taken from Rho et al. were also evaluated as a part of this project. The assignment criteria for trabecular bone are :

$$E_z = -331 + 4.56\ \rho \quad \text{and} \quad E_x = E_y = -581 + 3.77\rho \qquad \textbf{(5.3)}$$

For cortical bone the corresponding relationships are:

$$E_z = -6.142 + 0.014\ \rho \quad \text{and} \quad E_x = E_y = -5.05 + 0.0095\ \rho \qquad \textbf{(5.4)}$$

For Equations 5.3 all moduli are in MPa but for Equations 5.4 all moduli are in GPa. Density is in kg/m^3 in both cases. The results using these criteria are presented in Tables 5.3.5 and 5.3.6. Note that while the spread in $\epsilon 1$ is not significantly better than using the modified Carter Hayes criteria, the spread in $\epsilon 2$ is somewhat better. This is likely because the anisotropic nature of the bone is considered and taken into account. The disadvantage with this criteria is its complexity. Assigning direction dependent moduli requires significantly more computer memory and to compensate for this a coarser mesh must be used when applying these criteria to the full femur model. In the present context no significant gains were realized by using Rho et al. over Carter and Hayes.

Table 5.3.5: Comparison of calculated and experimental strains (in $\mu\epsilon$) for femur slice sections using unmodified Rho et al. criteria.

Slice	Finite Element		Experimental		% differences	
	$\epsilon 1$	$\epsilon 2$	$\epsilon 1$	$\epsilon 2$	$\epsilon 1$	$\epsilon 2$
T7_B10_B	-239	80	-419	152	43	47.4
T7_B10_S	-151	59	-207	131	27.1	55
T10_B13	-94	36	-106	87.5	11.3	58.9
T13_B16	-132	51	-217	76.2	39.2	33.1
T16_B19	-79	26	-113	83	30.1	68.7
T19_B22	-89	28	-136	37	34.6	24.3
T22_B25	-102	31	-156	46	34.6	32.6
average percent difference					31.4	45.7
standard deviation					10.3	16.2

Table 5.3.6: Comparison of calculated and experimental strains (in $\mu\epsilon$) for femur slice sections using linearly scaled Rho et al. criteria.

Slice	Finite Element		Experimental		% differences	
	$\epsilon 1$	$\epsilon 2$	$\epsilon 1$	$\epsilon 2$	$\epsilon 1$	$\epsilon 2$
T7_B10_B	-354	118	-419	152	15.5	22.4
T7_B10_S	-223	87	-207	131	-7.7	33.6
T10_B13	-139	53	-106	87.5	-31	39.4
T13_B16	-195	75	-217	76.2	10.1	1.57
T16_B19	-117	38	-113	83	-3.5	54.2
T19_B22	-132	41	-136	37	2.94	-11
T22_B25	-151	46	-156	46	3.21	0
average percent difference					-1.5	20.1
standard deviation					15.2	23.9

Because Carter and Hayes is simpler and requires less processing power it was chosen for use in the full femur model. This is not meant to be the final word on this issue. These results are based on only one femur and the Rho et al. criteria is certainly worthy of further investigation.

5.4 Full Femur (7mm mesh):

In this section FE results (calculated strains) from the full femur model (7mm mesh) will be compared with mechanical testing results (measured strains) for the full intact femur at seven locations detailed in Table 5.4.1. Material properties were assigned to the full femur model using a modified Carter Hayes relationship that was derived in Section 5.3.

$$E = 4421\rho^{2.5} \left(\frac{d\epsilon}{dt}\right)^{0.06} \qquad \textbf{(5.5)}$$

Calculated strains, experimental strains, and percent differences, as well as the calculated and measured principal angles (θ_p) are presented in Table 5.4.2.

The percent differences between measured and calculated strains for gage1 and gage2 are quite large (-200 and -105 respectively for $\epsilon 1$). The percent differences for the remaining gages are quite reasonable. Gage 1 and gage 2 are located high up on the head of the femur where the cortical shell is extremely thin. It is the strain in this very thin shell that is measured experimentally. From a FE modelling perspective, this thin shell is very

difficult to account for. Its radial dimension is so small compared to the dimension of the specimen, that modelling the shell accurately would require an extremely small and impractical mesh size. In short, hardware and software capabilities limit the degree of accuracy to which the cortical shell may be accounted for.

There are two probable causes for the large discrepancies at gage 1 and gage 2 and both relate to the FE model not accounting sufficiently for the thin cortical shell high up on the femoral head. Firstly, it is not well known how the load is actually shared between the trabecular and cortical bone in this region. Although the cortex is very thin it is also much stiffer and may play a significant structural role that is not accounted for in the FE model. This scenario implies that the actual femoral head region is stiffer than represented in the FE model. Secondly, experimental strains are measured on the outer surface of the cortex and may not be representative of actual strains below the surface. If so, the FE strains are a more accurate representation of reality than the experimentally measured strains. Further research is necessary to sort out what is actually going on in this region.

Table 5.4.1: Description of rosette strain gage locations.

Gage #	aspect	distance below femur ball (z = 0) in cm.
1	anterior	6.0
2	lateral	7.6
3	medial	12.7
4	anterior	12.0
5	lateral	12.7
6	anterior	24.1
7	lateral	24.1

Table 5.4.2: Comparison of FE strains ($\mu\epsilon$) and measured strains as well as principle angles (degrees) for full femur model (7 mm mesh, load = 70 kg).

	Finite Element			Experimental			% difference		diff
Gage#	$\epsilon 1$	$\epsilon 2$	θ_p	$\epsilon 1$	$\epsilon 2$	θ_p	$\epsilon 1$	$\epsilon 2$	$\Delta\theta_p$
1	-429	225	40	-143	124	29	-200	-81.5	-11
2	-137	246	21	-81	120	35	-69.1	-105	14
3	-351	169	12	-484	193	34	27.48	12.44	22
4	-71	217	28	-77	201	37	7.792	-7.96	9
5	-61	197	21	-50	168	41	-22	-17.3	20
6	-28	45	27	-37	87	43	24.32	48.28	16
7	-123	404	14	-164	402	30	25	-0.5	16

5.5 Full Femur (4.5mm mesh):

In this section results are presented (Table 5.5.1) comparing FE and experimental strains using a 4.5 mm FE mesh. The mesh was generated from the same set of solid model keypoints with points beyond z = 10 cm excluded. The motivation for this model is to verify convergence of the FE model and to better account for material property inhomogeniety in the proximal portion of the femur. Since the 7mm mesh had utilized software resources to full capacity (maximum allowable number of nodes) a smaller portion of the total femur was used to allow the application of a reduced mesh size. Gage locations four to seven are absent from the comparison in Table 5.5.1 because they are located beyond z = 10 cm on the femur shaft.

Table 5.5.1: Compaison of FE strains ($\mu\epsilon$) and measured strains as well as principle angles (degrees) for full femur model (4.5 mm mesh, load = 70 kg).

	Finite Element			Experimental			% difference		diff
Gage#	$\epsilon 1$	$\epsilon 2$	θ_p	$\epsilon 1$	$\epsilon 2$	θ_p	$\epsilon 1$	$\epsilon 2$	$\Delta\theta_p$
1	-282	173	27	-143	124	29	-97.2	-39.5	2.00
2	-105	123	38	-81	120	35	-29.6	-2.5	-3.00
3	-556	191	18	-484	193	34	-14.9	1.036	16.00

The smaller mesh size significantly reduced the percent errors in all three gage locations. This indicates that the model is converging (ie. approaching the actual solution as the mesh size becomes smaller). In addition these results support the notion that the thin

cortical shell might be structually significant since in this model the shell is accounted for to a greater extent. A mesh size of 2 mm or less would be needed to fully account for the cortical shell. One might suppose that a further reduction in mesh size would bring the FE and experimental results even closer.

CHAPTER 6

CONCLUSIONS AND RECOMMENDATIONS FOR FURTHER RESEARCH

6.1 FE Modelling:

This work has produced in-house technology for Memorial's Medical Engineering that can efficiently produce FE models of human femurs. The techniques will become faster and more efficient as research continues. Presently the technique can be summarized into five steps.

(1) Femur is CT scanned and the data transferred to Med Eng.

(2) Raw CT data is preprocessed by in-house software to a format compatible with FE

software.

(3) Femur geometry is recreated in ANSYS (FE software), for subsequent meshing into a FE model.

(4) Material properties are assigned to the model based on CT numbers and criteria developed for that particular specimen.

(5) Loads are applied and ANSYS calculates the stresses and strains.

During the course of developing this technology several significant contributions have been made to the field. First of all local technology, specific to the software and hardware resources at Memorial's Engineering have been developed, utilized and validated. At present it takes about five hours to model a femur from start to finish. There are no exact figures available for other techniques used elsewhere but generally the process is described as tedious and time consuming. There are other automated techniques described in Chapter 2 that are quite fast, such as (keyak et al., 1993). The most significant contribution of this modelling process is that the material properties are assigned on an element by element basis using criteria that are calibrated and validated for the specific bone being modelled. As far as the author is aware this has never been previously done. In addition to this, the boundary conditions have been applied in a manner that more closely match physiological loading conditions (Section 3.3). Previous studies generally used fixed boundary conditions along the shaft which never occurs in physiological loading.

Although progress has been made, there are challenges ahead. Improved CT image processing techniques will improve both the speed and geometric accuracy of FE models. Improvements in FE software (ie. upgrade from educational to commercial version) will allow finer meshes to be constructed. This will improve spatial resolution in terms of material properties. This is especially important since it will facilitate modelling of the thin cortex in the proximal region.

6.2 Mechanical Testing:

Significant contributions have been made to the mechanical testing of human femurs. First of all an environmental protocol has been established for the testing of human femurs (described in detail in Section 4.2). This will ensure consistency and reproducibility of results as well as provide material property data that is relevant to a specific test situation. Secondly, the femur has been tested in a configuration that is physiologically relevant (Section 4.4). The full intact femur was tested with no prior sectioning or potting. As far as the author is aware this has not been done before in the context of a FE study. Thirdly, a loading axis was defined that is both physiologically relevant and easily reproducible. This will also ensure reproducibility and consistency of results. If adopted as a standard it would do the same in an interlaboratory context. While progress has been made, further research is needed. Techniques need to be developed to apply muscle (abductor etc.) forces so that loading conditions can more

closely reflect physiological loads. The biggest challenges might be quite practical, such as attachment of load transfer mechanisms at appropriate locations. One suggestion might be to leave tendons in place and attach to them directly. Secondly, techniques must be found to measure strains under the surface of the bone. This will allow the validation of FE calculations at locations other than on the specimen's surface. Finally, and most importantly, more work is needed with a focus on material properties. Material properties are dependent on environmental factors post mortem as well as a host of other specimen specific factors. Little data is available in this area.

6.3 General Conclusions:

This study, in addition to establishing practical technology at Memorial's Medical Engineering Laboratory, has put FE modelling of the human femur on a firmer foundation. Good correlations between FE calculations and mechanical testing results have been achieved with loading conditions that are physiologically realistic. Modelling techniques are reasonably straight forward and may be applied by anyone with some introductory training in FE methods. Experimental techniques are well defined and may be easily reproduced. On the down side, these techniques were only applied to one femur. More work is needed on additional specimens to further validate the whole process and to learn more about the variation of material properties from one femur to another. Subsequent to further validation the modelling and testing techniques developed

here can be used on femurs with implants or other surgical alterations. In addition the modelling techniques may be used to compare the strain fields resulting from different implant types and orientations.

REFERENCES

Alberts, L.R., Pao, Y.C., and Lippiello, L. (1993). "A Large-Deformation, Finite Element Study of Chondrodiatasis in the Canine Distal Femoral Epiphyseal Plate," *Journal of Biomechanics,* Vol. 26, no. 11, pp.1291-1305.

Andriacchi, T.P., Galante, J.O., Belytschko, T.B., and Hampton, J.J. (1976). "A Stress Analysis of the Femoral Stem in Total Hip Prosthesis," *Journal of Bone and Joint Surgery,* Vol.58A, pp. 618-624.

Bartel, D.L., and McCarthy, M.A. (1990). "Structural Analysis of Bone-Implant Systems: The Effects of Modelling," *in Computational Methods in Bioengineering,* ed. R.I. Spiker, and B.R. Simon, pp. 199-210.

Beaupre, G.S., Orr, T.E., and Carter, D.R. (1990). "An Approach for Time-Dependent Bone Remodeling - Application: A Preliminary Remodeling Simulation," *Journal of Orothopaedic Research,* Vol. 8, pp. 662-670.

Bobyn, J.D., Mortimer, E.S., Glassman, A.H., Engh, C.A., Miller, J.E., and Brooks, C.E. (1992). "Producing and Avoiding Stress Shielding," *Clinical Orthopaedics and Related Research,* no. 274, pp.79-96.

Brockhurst, P. (1975). "Design for Total Hip Prosthesis - The Femoral Stem," *Center for Biomedical Engineering Report,* University of N.S.W., July

Burke, D.W., Davies, J.P., O'Connor, D.O., and Harris, W.H. (1984). "Experimental Strain Analysis in the Femoral Cement Mantle of Simulated Total Hip Arthoplasties," *Transactions of the 30th Annual Meeting of the Orthopaedic Research Society,* pp. 296.

Carlsson, L., Albrektsson, B., and Freeman, M.A.R. (1988). "Femoral Neck Retention in Hip Arthroplasty," *Acta Orthop Scand,* Vol. 59, pp. 6-8.

Carter, D.R., Hayes, W.C. (!977). "The Compressive Behavior of Bone as a Two-Phase Porous Structure," *Journal of Bone and Joint Surgery,* Vol. 59A, pp. 954-962.

Carter, D.R., Hayes, W.C. (1976). "Bone Compressive Strength: The Influence of Density and Strain Rate,"*Science,* Vol. 194, pp. 1174-1176.

Carter, D.R., Orr, T.E. and Fyhrie, D.P. (1989). "Relationships Between Loading History and Femoral Cancellous Bone Architecture," *Journal of Biomechanics,* Vol. 22, no. 3, pp. 231-244.

Edidlin, A.A, Taylor, D.L., Bartel, D.L. (1991). "Automatic Assignment of Bone Moduli From CT Data: A 3-D Finite Element Study," *Transactions of th 37th Annual Meeting, Orothopaedic Research Society,* Anaheim, California, pp. 491.

Evans, F.G., and King, A.T. (1961). "Regional Differences in Some Physical Properties of Human Spongy Bone," *in Biomechanical Studies of the Musculo-Skeletal System,* ed. Evans, F.G., Springfield, Illinois, pp. 49-67.

Fyhrie, D.P., and Schaffler, M.B. (1995). "The Adaptation of Bone Apparent Density to Applied Load," *Journal of Biomechanics,* Vol. 28, no. 2, pp. 135-146.

Goldstein, S.A. (1987). "The Mechanical Properties of Trabecular Bone: Dependance on Anatomical Location and Function," *Journal of Biomechanics,* Vol. 20, pp. 1055-1061.

Hampton, S.J., Andriacchi, T.P., and Galante, J.O. (1980). "Three Dimensional Stress Analysis Of the Femoral Stem of a Total Hip Prosthesis," *Journal of Biomechanics*, Vol. 13, pp443-448.

Hampton, S.J., and Andriacchi, T.P. (1979). "An Analytical Representation of the Non-Linear Interface Condition in a Bone-Cement-Prosthesis System," *Intenational Conference on Finite Elements in Biomechanics,*ed. B.R. Simon, pp.193-206.

Harrigan, T.P., and Harris, W.H. (1991). "A Three-Dimensional Non-Linear Finite Element Study of the Effect of Cement-Prosthesis Debonding in Cemented Femoral Total Hip Components," *Journal of Biomechanics*, Vol. 24, pp. 1047-1058.

Harrigan, T.P., and Harris, W.H. (1991). "A Finite Element Study of the Effect of Diametral Interface Gaps on the Contract Areas and Pressures in Uncemented Cylindrical Femoral Total Hip Components," *Journal of Biomechanics*, Vol. 24, pp. 87-91.

Harrigan, T.P., Kareh, J.A., O'Conner, D.O., Burke, D.W., and Harris, W.H. (1992). "A Finite Element Study of the Initiation of Failure of Fixation in Cemented Femoral Total Hip Components," *Journal of Orthopaedic Research,* Vol. 10, no. 1, pp. 134-144.

Huiskes, R., Janssen, J.D., and Slooff, T.J. (1981). "A Detailed Comparison of Experimental and Theoretical Stress Analysis of a Human Femur," *in Mechanical Properties of Bone,* ed. S. Cowin, American Society of Mechanical Engineers, New York, Vol. 45, pp. 211-234.

Huiskes, R. (1990). "The Various Stress Patterns of Press-Fit, Ingrown, and Cemented Femoral Stems,"*Clinical Orthopaedics and Related Research,* no. 261, pp. 27-38.

Huiskes, R., Weinans, H., and Van Rietbergen, B. (1992). "The Relationship Between Stress Shielding and Bone Resorption Around Total Hip Stems and the Effects of Flexible Materials," *Clinical Orothopaedics and Related Research,* no. 274, pp. 124-134.

Jansson, V., Heimkes, B., and Zimmer, M. (1993). "Stress Transfer at the Bone / Bone Cement Interface as a Function of the Cement Thickness," *Archives of Orthopaedic and Trauma Surgery,* Vol. 112, pp. 65-68.

Kang, Y.C., Park, H.C., Youm, Y., Lee, I.K., Ahn, M.H., and Ihn, J.C. (1993). "Three Dimensional Shape Reconstruction and Finite Element Analysis of Femur Before and After the Cementless Type of Total Hip Replacement," *Journal of Biomedical Engineering,* Vol. 15, pp. 497-504.

Keavney, T.M., and Bartel, D.L. (1993). "Effects of Porous Coating and Collar Support on Early Load Transfer for a Cementless Hip Prosthesis," *Journal of Biomechanics,* Vol. 26, no. 10, pp.1205-1216.

Keavney, T.M., and Bartel, D.L. (1994). "Fundamental Load Transfer Patterns for Press-Fit, Surface Treated Intramedullary Fixation Stems," *Journal of Biomechanics,* Vol. 27, no. 9, pp.147-1157.

Keavney, T.M., and Bartel, D.L. (1993). "Load Transfer with the Austin Moore Cementless Hip Prosthesis," *Journal of Orothopaedic Research,* Vol. 11, pp. 272-284.

Keyak, J.H., Meagher, J.M, Skinner, H.B. and Mote, C.D. (1990). "Automated Three Dimensional Finite Element Modelling of a Bone: A New Method," *Journal of Biomedical Engineering,* Vol. 12, pp. 389-397.

Keyak, J.H., Fourkas, M.G., Meagher, J.M., and Skinner, H.B. (1993). "Validation of an Automated Method of Three Dimensional Finite Element Modelling of Bone," *Journal of Biomedical Engineering,* Vol. 15, pp.505-509.

Kwak, B.M. Lim, O.K., Kim, Y.Y., and Rim, K. (1979). "An Investigation of the Effect of Cement Thickness on an Implant by Finite Element Stress Analysis," *International Orthopaedics,* Vol. 2, pp. 315-319.

Lee, D.G.Y. (1995). "Material Properties of Bone" *Unpublished Paper, Medical Engineering Laboratory,* Memorial University of Newfoundland, St. Johns, Newfoundland, Canada.

Lengsfeld, M., Kaminsky, J., Merz, B., and Franke, R.P. (1994). "Automatisierte Generierung von 3-D Finite Elemente Codes des Menschlichen Femurs," *Biomed Technik,* Vol. 39, pp. 117-122.

Leone, D., Breglia, L., Gander, J., Ibets, J., Teeling, C., and Lewis, C. (1990). "Total Hip Arthroplasty - Finite Element Analysis Validation," *Proceedings of the 16th Annual Northeast Bioengineering Conference,* IEEE, pp. 3-4.

Lewis, C.G., Leone, D.J., Nowak, M.D., Davis, P.A., and Huang, S.J. (1991). "Expeimental Validation of Three Dimensional Finite Element Analysis in Total Hip Arthroplasty,"Transactions of the *37th Annual Meeting, Orthopaedic Research Society,* Anaheim, California, pp. 515.

Lewis, J.L., Kramer, G.M., Wixson, R.L., and Askew, M.J. (1981). "Calcar Loading by Titanium Total Hip Stems," *Transactions of the 27th Annual Meeting of the Orthopaedic Research Society,* Vol. 6, pp. 75.

Lotz, J.C., Cheal, E.J., and Hayes, W.C. (1991). "Fracture Prediction for the Proximal Femur Using Finite Element Models: Part II - Nonlinear Analysis," *Journal of Biomechanical Engineering,* Vol. 113, pp. 361-365.

Lotz, J.C., Cheal, E.J., and Hayes, W.C. (1991). "Fracture Prediction for the Proximal Femur Using Finite Element Models: Part I - Linear Analysis," *Journal of Biomechanical Engineering,* Vol. 113, pp. 353-360.

Martin, R.B. (1984). "Porosity and Specific Surface of Bone," *CRC Critical Reviews in Biomedical Engineering,* Vol. 10, pp. 179-222.

McElhaney, J.H, Foyle, J.L., Melvin, J.W., Haynes, R.R., Roberts, V.L., and Alem, N.M. (1970). "Mechanical Properties of Cranial Bone," *Journal of Biomechanics,* Vol. 3, pp. 495-511.

Measurement Group INC. (1983). Bulletin 309, Raleigh, North Carolina.

O'Connor, D., Burke, D.W., Jasty, M., Sedlace, R.C., and Harris, W.H. (1996). "In Vitro Measurement of Strain in the Bone Cement Surrounding the Femoral Component of Total Hip Replacements during Simulated Gait and Stair-Climbing,"*Journal of Orthopaedic Research,* Vol. 14, no. 5, pp. 769-777.

Pugh, J.W., Rose, R.M., Radin,E.L., (1973). "Elastic and ViscoElastic Properties of Trabecular Bone: Dependence on Structure," *Journal of Biomechanics,* Vol. 6, pp. 475-485.

Rho, J.Y., Hobatho, M.C., and Ashman, R.B. (1995). "Relations of Mechanical Properties to Density and CT numbers in Human Bone," *Med. Eng. Phys,* Vol. 17, no. 5, pp. 347-355.

Rohlmann, A., Mossner, U., Bergmann, G., and Kolbel, R. (1983). "Finite Element Analysis and Experimental Investigation in a Femur With Hip Endoprosthesis," *Journal of Biomechanics,* Vol. 16, no. 9, pp. 727-742.

Rohlmann, A., Bergmann, G., and Kolbel, R. (1982). "The Relevance of Stress Computation in the Femur With and Without Endoprostheses," in *Finite Elements in Biomechanics,* ed. R.H. Gallagher, B.R. Simon, P.C. Johnson, and J.F. Gross, John Wiley, Chichester, pp. 361-378.

Schaffler, M.B., and Burr, D.B. (1988). "Stiffness of Compact Bone: Effects of Porosity and Density," *Journal of Biomechanics,* Vol. 21, no. 1, pp. 13-16.

Schmalzried, T.P., Kwong, L.M., Jasty, M., Sedlacek, R.C., Haire, T.C., O'Connor, D.O., Bragdon, C.R., Kabo, J.M., Malcolm, A.J., Path, M.R.C., and Harris, W.H. (1992). "The Mechanical Loosening of Cemented Acetabular Components in Total Hip Arthroplasty," *Clinical Orthopaedics and Related Research,* no. 274, pp. 60-78.

Skinner, H.B., Kim, A.S., Keyak, J.H., and Mote, C.D. (1994). "Femoral Prosthesis Implantation Induces Changes in Bone Stress that Depend on the Extent of Porous Coating," *Journal of Orothopaedic Research,* Vol. 12, pp. 553-563.

Skinner, H.B., Kilgus, D.J., Keyak, J., Shimaoka, E.E., Kim,A.S., and Tipton, J.S. (1994). "Correlation of Computed Finite Element Stresses to Bone Density After Remodeling Around Cementless Femoral Implants," *Clinical Orothopaedics and Related Research,* no. 305, pp. 178-189.

Sumner, D.R., and Galante, J.O. (1992). "Determinants of Stress Sheilding: Design Versus Materials Versus Interface," *Clinical Orothopaedics and Related Research,* no. 274, pp. 203-212.

Svesnsson, N.L., Valliappan, S., and Wood, R.D. (1977). "Stress Analysis of Human Femur With Implanted Charnley Prosthesis," *Journal of Biomechanics,* Vol. 10, pp. 581-588.

Tanner, K.E., Yettram, A.L., Loeffler, M., Goodier, W.D., Freeman, M.A.R., and Bonfield, W. (1995). "Is Stem Length Important In Uncemented Endoprostheses," *Medical Engineering Physics,* Vol. 17, no. 4, pp. 291-296.

Tanner, K.E., Bonfield, W., Nunn, D. And Freeman, M.A.R. (1988). "Rotational Movement of Femoral Components of Total Hip Replacements in Response to an Anteriorly Applied Load," *Engineering Medicine,* Vol. 17, no. 3, pp. 127-129.

Tarr, R., Lewis, J., Ghassemi, F., Sarmiento, A., Clarke, I., and Weingarten, V. (1980). "Anatomic Three Dimensional Finite Element Model of the Proximal Femur With Total Hip Prosthesis," *International Conference Proceedings, Finite Elements in Biomechanics,* ed. B.R. Simon, The University of Arizona, Tuscon, Vol. 2, pp. 511- 525.

Valliappan, S., Svensson, N.L., and Wood, R.D., (1977). "Three Dimensional Stress Analysis of the Human Femur," *Computing in Biology and Medicine,* Vol. 7, pp. 253-264.

Van Rietbergen, B., Huiskes, R., Weinans, H., Sumner, D.R., Turner, T.M., and Galante, J.O., (1993). "The Mechanism of Bone Remodelling and Resorption Around Press-Fitted THA Stems," *Journal of Biomechanics,* Vol. 26, no. 4/5, pp. 369-382.

Verdonschot, N.J.J., Huiskes, R., and Freeman, M.A.R. (1993). "Pre-Clinical Testing of Hip Prosthetic Designs: A Comparison of Finite Element Calculations and Laboratory Tests," *Proceedings of the Institution of Mechanical Engineers. Part H, Journal of Engineering in Medicine,* Vol. 207, no. 3, pp. 149-154.

Weinans, H., Huiskes, R., and Grootenboer, H.J. (1994). "Effects of Fit and Bonding Characteristics of Femoral Stems on Adaptive Bone Remodeling," *Transactions of the* ASME: *Journal of Biomechanical Engineering*, Vol. 116, pp. 393-400.

Yoon, Y.S., Jang, G.H., and Kim, Y.Y. (1989). "Shape Optimal Design of th Stem of a Cemented Hip Prosthesis to Minimize Stress Concentration in the Cement Layer," *Journal of Biomechanics,* Vol. 22, no. 11/12, pp. 1279-1284.

APPENDIX A

Automated Model Building

Dawna Greening, a graduate student working in the Biomedical Engineering Centre at Memorial University of Newfoundland, has written a series of computer programs to assist the user in building a 3-D solid model of the human femur. The programs perform a series of tasks in an attempt to automate the model building process as much as possible. The first step is the transfer of raw CT data from diskette to the processing computer in the laboratory. At this stage, each file is assigned a unique name indicating the associated scan and slice number. Formatting differences between the CT data collection and processing computers requires that the CT data be translated into a compatible format before further processing can be performed. During this translation stage, the images are also cropped to exclude all extraneous data other than bone. These smaller images, or regions-of-interest (ROI's), require less storage space, and can be processed more quickly. Working with these ROI's, the user specifies a range of CT values that may be considered cortical bone. A thresholding technique is then used to extract the perimeter edges of the cortical bone, and the resulting edge points are written to a file, by default, in a row-wise fashion. To enable quick selection of equidistant points along the edges, these stored perimeter data points are re-sorted, placing adjacent edge points next to each other in the data file. With the points sorted in this manner, a user-specified number of

equidistant points is easily placed along the edges by selecting equidistant points from the sorted listing of edge points. All slice data is displayed showing the selected points, and the user has the option of making changes using a graphical point editor. When satisfied that the point placements are correct, an ANSYS input file is automatically generated to plot keypoints, draw splines, skin over areas and generate a solid volume model of the femur.

APPENDIX B

Details on 75% Humidity Source

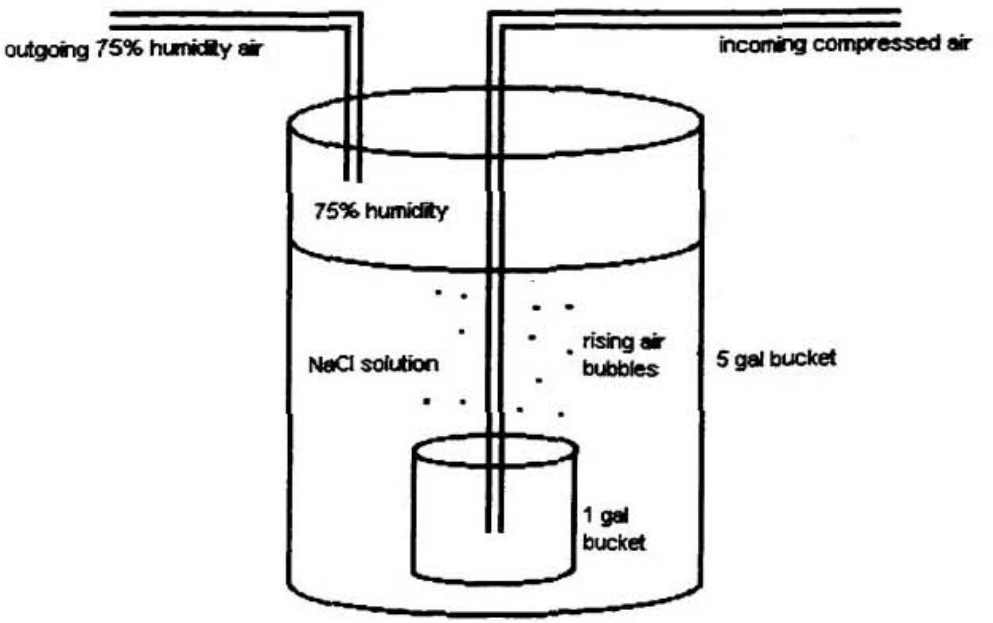

The humidity above a concentrated Sodium Chloride solution is relatively constant at about 75% (Handbook of Chemistry and Physics, 74th edition, pp. 15-25). It follows that if air is bubbled through a NaCl solution the resulting air will be at 75% humidity as long as the air solution contact is sufficient. The figure above depicts the device used in this project to supply 75% humidity air.

The basic design consisted of a one gallon plastic bucket nested upside down inside a five

gallon plastic bucket. The five gallon bucket had a sealed plastic lid and the one gallon bucket had fifty 1/4 inch holes drilled in its bottom. The larger bucket was filled about 3/4 full of concentrated NaCl solution. Compressed air was piped into the smaller bucket at a controlled rate. The air bubbles were dispersed through the holes in the smaller bucket and picked up moisture as they rose to the top of the NaCl solution. The resulting trapped 75% humidity air was vented off to the environmental chamber that enclosed the experiment via a plastic hose inserted into the lid of the larger bucket. This apparatus was tested to insure that the vented air was at 75% humidity for the air flow rate that was used in the experiments.

APPENDIX C

Details on Strain Gage Attachment

Memorial's Medical Engineering has adapted a procedure for the attachment of strain gages to bone from a standard attachment procedure outlined by Measurements Group who supply strain gage technology and hardware (Measurements Group ,1983).

The area of the bone to which the gage was attached was thoroughly cleaned down to the cortical shell. All soft tissue (ie.cartilage and muscle) was removed. This was difficult at muscle attachment sites such as the greater throchanter where the transition from tendon to bone is gradual with no well defined boundary. A similar problem also exists at joint locations (ie. head of femur and condyles) where the transition from cartilage to bone is gradual. These difficulties restrict where strain gages may be successfully attached.

After initial cleaning the attachment site was thoroughly degreased with Chlorothene SM™ (Measurements Group, Inc. Raleigh, USA) and then dry abraded with 320 grit silicon carbide-paper. Next the surface was wetted with M-Prep Conditioner™ (Measurements Group, Inc. Raleigh, USA) and wet abraded with 320 or 400 grit silicon-carbide. After drying with tissue paper the wet abrading process was repeated. Next the exact gage location was marked with a pencil and the surface was wetted again with M-

Prep Conditioner™ and dried. Finally the surface was neutralized with M-Prep Neutralizer 5™ (Measurements Group, Inc. Raleigh, USA) and dryed off with tissue paper. The gages were aatached to the prepared surfaces using M-Bond 200™ adhesive and M-Bond 200™ catalyst (Measurements Group, Inc. Raleigh, USA).

APPENDIX D

Physiology of the Human Femur

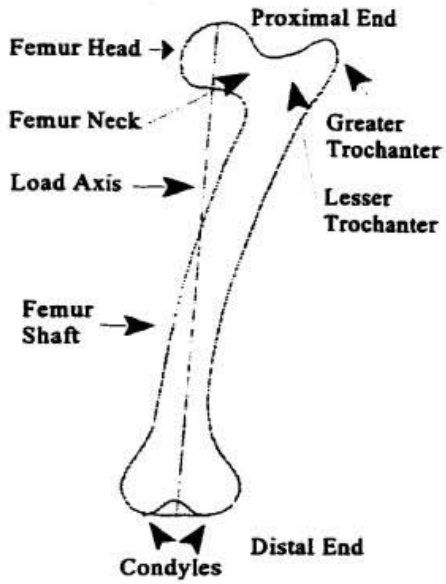

The purpose of this Appendix is to familiarize the reader with the terminologies used in reference to the human femur in the context of this thesis. The femur (depicted in figure above) or thighbone is the longest and heaviest bone in the human body. The end of the femur closest to the hip joint is called the proximal end and the end towards the knee is called the distal end. If one strain gage is attached 2.0 cm distal to another it simply means that the gage is located 2.0 cm further towards the knee joint.

At the proximal end of the femur there is a ball shaped protrusion called the femoral head. This head articulates (connects) with the coxal bone to form the hip joint. The neck of the femur is a constricted region distal to the head. This is the region that typically fractures in older people and necessitates total hip replacement. The greater trochanter and the lesser trochanter are projections that serve as muscle attachment sites for some of the thigh and buttock muscles. The shaft of the femur is a relatively uniform and essentially cylindrical region distal to the head and proximal to the condyles. The condyles are two rounded protrusions at the distal end of the femur that articulate with the tibia (shinbone) to form the knee joint.

There are also specific terminologies used to refer to aspects of the femur in reference to larger scale orientations of the human body. The lateral side of the femur faces outwards to the side of the human body. The medial side faces inwards towards the inner thigh. Prosterior and anterior refers to toward the back and towards the front of the body respectively.

The femur is composed of both cortical (compact) and trabecular (spongy or cancellous) bone. Cortical bone is the more dense higher modulus material that forms the outer shell or cortex of the femur. It is thinner near the ends of the femur and thicker in the shaft where it is needed to resist bending moments. Trabecular bone is a less dense spongy or honeycombed material that composes the interior of the head and condyles of the femur.

BIBLIOGRAPHY

Andriacchi, T.P., Galante, J.O., Belytschko, T.B., and Hampton, S. (1976). "A Stress Analysis of the Femoral Stem in Total Hip Prostheses," *The Journal of Bone and Joint Surgery,* Vol. 58A, no. 5, pp. 618-624.

Andrisano, A.O., Dragoni, E., and Strozzi, A. (1990). "Axisymmetric Mechanical Analysis of Ceramic Heads for Total Hip Replacement," *Journal of Engineering in Medicine,* Vol. 204, no. 3, pp. 157-167.

Ashman, R.B., Cowin, S.C., Van Buskirk, W.C., and Rice, J.C. (1984). " A Continuous Wave Technique For the Measurement of th Elastic Properties of Cortical Bone," *Journal of Biomechanics,* Vol. 17, no. 5, pp. 349-361.

Bay, B. (1995). "Texture Correlation: A Method for the Measurement of Detailed Strain Distributions Within Trabecular Bone," *Journal of Orthopaedic Research,* Vol. 13, no. 2, pp. 258-267.

Bechtold, J.E., and Riley, D.R. (1991). "Application of Beams on Elastic Foundations and B-Spline Solution Methodologies to Parametric Analysis of Intramedullary Implant Systems," *Journal of Biomechanics,* Vol. 24, no. 6, pp. 441-448.

Boden, S.D., Goodeough, D.J., Stockham, C.D., Jacobs, E., Dina, T., and Allman, R.M. (1989). "Precise Measurement of Vertebral Bone Density Using Computed Tomography Without the Use of an External Reference Phantom," *Journal of Digital Imaging,* Vol. 2, no. 1, pp. 31-38.

Bozic, K.J., Keyak, J.H., Skinner, H.B., Bueff, H.U., and Bradford, D.S. (1994). "Three-Dimensional Finite Element Modeling of a Cervical Vertrbra: An Investigation of a Burst Fracture Mechanism," *Journal of Spinal Disorders,* Vol. 7, no. 2, pp. 102-110.

Broz, J.J., Simske, S.J., and Greenberg, A.R. (1995). "Material and Compositional Properties of Selectively Demineralized Cortical Bone," *Journal of Biomechanics,* Vol. 28, no. 11, pp. 1357-1368.

Burton, D.S, and Skinner, H.B. (1989). "Stress Analysis of a Hip Acetabular Component: An FEM Study," *Biomaterials, Artificial Cells, Artificial Organs,* Vol. 17, no. 4, pp. 371-383.

Cheal, E.J., Spector, M., and Hayes, W.C. (1992). "Role of Loads and Prosthesis Material Properties on the Mechanics of the Proximal Femur After Total Hip Arthroplasty," *Journal of Orthopaedic Research,* Vol. 10, no. 3, pp. 405-422.

Cristfolini, L., Viceconti, M., Capello, A. and Toni, A. (1996). "Mechanical Validation of Whole Bone Composite Femur Models," *Journal of Biomechanics,* Vol. 29, no. 4, pp. 525-535.

Crowninshield, R.D., Brand, R.A., and Johnston, R.C. (1990). "An Analysis of Femoral Component Stem Design in Total Hip Arithroplasty," *The Journal of Bone and Joint Surgery,* Vol. 62A, no. 1, pp. 68-78.

Dragoni, E., and Andrisano, A.O. (1995). "Structural Evaluation of Ceramic Femoral Heads: Effect of Taper Friction, Support Conditions and Trunnion Compliance," *Journal of Biomechanical Engineering,* Vol. 117, no. 3, pp. 293-299.

Engh, C.A., McGovern, T.F., and Schmidt, L.M.(1993). "Roentgenographic Densitometry of Bone Adjacent to a Femoral Prosthesis," *Clinical Orthopaedics and Related research,* No. 292, pp. 177-190.

Fyhrie, D.P., and Carter, D.R. (1990). "Femoral Head Apparent Density Distribution Predicted From Bone Stresses," *Journal of Biomechanics,* Vol. 23, no. 1, p. 1-10.

Gibson, L.J. (1985). "The Mechanical Behaviour of Cancellous Bone," *Journal of Biomechanics,* Vol. 18, no. 5, pp. 317-328.

Goldstein, S.A. Ku, J.L., Hollister, R., Goulet, F.W., and Matthews, L.S. (1987). "Experimentally Controled Trabecular Bone Remodelling: Effects of Applied Stress," *Transactions of the 33rd Annual Meeting, Orthopaedic Research Society,* San Francisco, California, pp. 461.

Goulet, R.W., Goldstein, S.A, Ciarelli, M.J., Kuhn, J.L., Brown, M.B., and Feldkamp, L.A. (1994). "The Relationship Between the Structural and Orthogonal Compressive Properties of Trabecular Bone," *Journal of Biomechanics,* Vol. 27, no. 4, pp. 375-389.

Hampton, S.J., Andriacchi, T.P., Draganich, L.F., and Galante, J.O. (1981). "Stresses Following Stem Cement Bond Failure if Femoral Total Hip Implants," *Transactions of the 27th Annual Meeting of the Orthopaedic Research Society,* pp. 144.

Hubsch, P.f., Middleton, J., Meroi, E.A., and Natali, A.N. (1995). "Adaptove Finite-Element Approach for the Analysis of Bone/Prosthesis Interaction," *Medical and Biological Engineering and Computing,* Vol. 33, no. 1, pp. 33-37.

Huiskes, R. and Rietbergen, B. (1985) "Preclinical Testing of Total Hip Stems: The Effects of Coating placement," *Clinical Orthopaedics and Related Research,* Vol. 319, pp. 64-76.

Huiskes, R., Weinans, W., and Dalstra, M. (1989). "Adaptive Bone Remodeling and Biomechanical Design Considerations: for Noncemented Total Hip Arthroplasty," *Orthopaedics,* Vol. 12, no. 9, pp. 1255-1267.

Huiskes, R. (1983). "A Survey of Finite Element Analysis in Orthopaedic Biomechanics: The First Decade," *Journal of Biomechanics,* Vol. 16, pp. 385-407.

Huiskes, R., and Boeklagen, R. (1989). "Mathematical Shape Optimization of Hip Prosthesis Design," *Journal of Biomechanics,* Vol. 22, pp. 793-804.

Jacob, H.A.C., and Huggler, A.H. (1980). "An Investigation into Biomechanical Causes of Prosthesis Stem Loosening Within the Proximal End of the Human Femur," *Journal of Biomechanics,* Vol. 13, pp. 159-173.

Keavney, T.M., Pinilla, T.P., Crawford, P., and Wachtel, E.F. (1995). "Improved Techniques for the Mechanical Testing of Human Trabecular Bone," *Transactions of Orthopaedic Research Society,* pp. 530.

Keavney, T.M., and Hayes, W.C. (1993). "A 20-Year Perspective on the Mechanical Properties of Trabecular Bone," *Journal of Biomechanical Engineering,* Vol. 115, pp. 534-542.

Kuiper, J.H., and Huiskes, R. (1996). "Friction and Stem Stiffness Affect Dynamic Interface Motion in Total Hip Replacement," *Journal of Orthopaedic Research: Official Publication of the Orthopaedic Research Society,* Vol. 14, pp. 36-43.

Laird, G.W., and Kingsbury, H.B. (1973). "Complex Viscoelastic Moduli of Bovine Bone," *Journal of Biomechanics,* Vol. 6, pp.59-67.

Lee, I.Y., Skinner, H.B., and Keyak, J.H. (1994). "Effects of Variation of Prosthesis Size on Cement Stress at the Tip of the Femoral Implant," *Journal of Biomedical Materials Research,* Vol. 28, pp. 1055-1060.

Lee, I.Y., Skinner, H.B., and Keyak, J.H. (1993). "Effects of Variation of Cement Thickness on Bone and Cement Stress at the Tip of the Femoral Implant," *The Iowa Orthopaedic Journal,* Vol. 13, pp. 155-159.

Liao, K. (1994). "Performance Characterization and Modeling of a Composite Hip Prosthesis," *Experimental Techniques,* Iss. September/October, pp. 33-38.

Lotz, J.C., and Hayes, W.C. (1990). "The Use of Quantitative Computed Tomography to Estimate Risk of Fracture of the Hip from Falla," *The Journal of Bone and Joint Surgery,* Vol. 72A, pp. 689-699.

Mann, K.A., Bartel, D.L., Wright, T.M., and Burstein, A.H. (1995). "Coulomb Frictional Interfaces in Modeling Cemented Total Hip Replacements: A More Realistic Model," *Journal of Biomechanics,* Vol. 28, no. 9, pp. 1067-1078.

Mann, K.A., Bartel, D.L., Wright, T.M., and Ingraffea, A.R. (1991). "Mechanical Characteristics of the Stem-Cement Interface," *Journal of Orthopaedic Research,* Vol. 9 pp. 798-808.

Markolf, K.L, and Amstutz, H.C. (1976). "A Comparative Experimental Study of Stresses in Femoral Total Hip Replaceent Components: The Effects of Prostheses Orientation and Acrylic Fixation," *Journal of Biomechanics,* Vol. 9, pp. 73-79.

Martin, R.B., Papamichos, T., and Dannucci, G.A. (1990). "Linear Calibration of Radiographic Mineral Density Using Video-Digitizing Methods," *Calcified Tissue International,* Vol. 47, pp. 82-91.

Messersmith, P.B., and Cooke, F.W. (1990). "Stress Enhancement and Fatigue Susceptibility of Porous Coated Tl-6Al-4V Implants; and Elastic Analysis," *Journal of Biomedical Material Research,* Vol. 24, pp. 591-604.

Offut, C.J., Vannier, M.W., Gilula, L.A., Marsh, J.L., and Sutherland, C.J. (1990). "Volumetric 3-D Imaging of Computerized Tomography Scans," *Radiologic Technology,* Vol. 61, pp. 212-219.

Poss, R. (1992). "Natural Factors That Affect the Shape and Strength of the Aging Human Femur," *Clinical Orthopaedics and Related Research,* No. 274, pp.194-201.

Prendergast, P.J., and Taylor, D. (1990). "Stress Analysis of the Proximo-Medial Femur After Total Hip Replacement," *Journal of Biomedical Engineering,* Vol. 12, pp. 379-382.

Quesnel, T., Gueritey, P.M., and Gonon, G.P. (1995). "Biomechanics of the Hip: Forces Exerted During Walking," *Surgical and Radiologic Anatomy,* Vol. 17, no. 3, pp. 249-253.

Reilly, D., and Burstein, A.H. (1975). "The Elastic and Ultimate Properties of Compact Bone Tissue," *Journal of Biomechanics,* Vol. 8 pp. 393-405.

Rotem, A. (1994). "Effect of Implant Material Properties on the Performance of a Hip Joint Replacement," *Journal of Medical Engineering and Technology,* Vol. 18, no. 6, pp. 208-217.

Rubin, P.J., Rakotomamana, R.L., Leyvraz, P.F., Zysset, P.K., Curnier, A., and Heegard, J.H. (1993). "Frictional Interface Micromotions and Anisotropic Stress Distribution in a Femoral Total Hip Component," *Journal of Biomechanics,* Vol. 26, pp. 725-734.

Shirandami, R., and Esat, I.I. (1990). "New Design of Hip Prosthesis Using Carbon Fibre Reinforced Composite," *Journal of Biomedical Engineering,* Vol. 12, no. 1, pp. 19-22.

Simkin, A., and Robin, G. (1973). "The Mechanical Testing of Bone in Bending," *Journal of Biomechanics,* Vol. 6, pp. 31-39.

Taylor, M., Tanner, K.E., Freeman, M.A.R., and Yettram, A.L. (1995). "Cancellous Bone Stresses Surrounding the Femoral Component of a Hip Prosthesis: An Elastic-Plastic Finite Element Analysis," *Medical Engineering and Physics,* Vol. 17, no. 7, pp. 544-550.

Tensi, H.M., Gese, H., and Ascherl, R. (1989). "Non-linear Three-Dimensional Finite Element Analysis of a Cementless Hip Endoprosthesis," *Journal of Engineering in Medicine,* Vol. 203, no. 4, pp. 215-222.

Turner, C.H., and Cowin, S.C. (1988) "Errors Induced by Off-Axis Measurement of the Elastic Properties of Bone." *Journal of Biomechanical Engineering,* Vol. 110, pp. 213-215.

Weinstein, A.M., Koeneman, J.B., and Hansen, T.M. (1987). "Finite Element Analysis of a Composite Material Hip Stem," *Transactions: Thirteenth Annual Meeting of the Society for Biomaterials*, New York, New York, U.S.A., Iss. June 3-7, pp. 264.